ESTCP
Cost and Performance Report

(MM-0607)

Wide Area UXO Screening with the Multi-Sensor Fixed-wing Airborne System MARS, Former Kirtland Precision Bombing Range, NM

June 2008

ENVIRONMENTAL SECURITY
TECHNOLOGY CERTIFICATION PROGRAM

U.S. Department of Defense

COST & PERFORMANCE REPORT
Project: MM-0607

TABLE OF CONTENTS

Page

1.0 EXECUTIVE SUMMARY ix

2.0 INTRODUCTION 1
- 2.1 BACKGROUND 1
- 2.2 OBJECTIVES OF THE DEMONSTRATION 1
- 2.3 REGULATORY DRIVERS 2

3.0 TECHNOLOGY 3
- 3.1 TECHNOLOGY DESCRIPTION 3
  - 3.1.1 Airborne Platform 3
  - 3.1.2 Airborne Sensors and Boom 3
  - 3.1.3 Positioning Technologies 4
  - 3.1.4 Development and Prior Testing of the Technology 4
- 3.2 ADVANTAGES AND LIMITATIONS OF THE TECHNOLOGIES 7

4.0 PERFORMANCE OBJECTIVES 9

5.0 SITE DESCRIPTION 11
- 5.1 SITE LOCATION AND HISTORY 11
- 5.2 SITE GEOLOGY 11
- 5.3 MUNITIONS CONTAMINATION 11
- 5.4 PRE-DEMONSTRATION TESTING AND ANALYSIS 11

6.0 TEST DESIGN 13
- 6.1 CONCEPTUAL EXPERIMENTAL DESIGN 13
- 6.2 SITE PREPARATION 13
- 6.3 SYSTEM SPECIFICATION 13
- 6.4 DATA COLLECTION 13
- 6.5 VALIDATION 15

7.0 DATA ANALYSIS AND PRODUCTS 19
- 7.1 PREPROCESSING 19
- 7.2 TARGET SELECTION FOR DETECTION 20
- 7.3 DATA PRODUCTS 20

8.0 PERFORMANCE CONFIRMATION METHODS 21
- 8.1 PERFORMANCE CONFIRMATION METHODS 21
- 8.2 DETECTION PROBABILITY RELATIVE TO HELIMAG 24

TABLE OF CONTENTS (continued)

Page

9.0 COST ASSESSMENT 31
9.1 COST MODEL 31
9.2 COST DRIVERS 31
9.3 COST BENEFIT 33

10.0 REFERENCES 37

APPENDIX A POINTS OF CONTACT A-1
APPENDIX B SELECTED IMAGES OF GROUND, MARS, AND HELIMAG DATA B-1

LIST OF FIGURES

Page

Figure 1. The CT SW Light Sport Aircraft Collecting Data at the Former Kirtland Precision Bombing Range. 1
Figure 2. Schematic of the MARS Sensor Layout. 5
Figure 3. Former Kirtland Precision Bombing Range with Identified Bombing Targets and other Areas of Interest, Including Existing Features and the Utilities Infrastructure. 12
Figure 4. Results of Daily Calibrations (with different days plotted as different symbols, and each calibration item as a different color). 16
Figure 5. (a) Best and Worst Case Anomaly Amplitudes for the 81-mm Mortar, 105-mm HEAT Round, and the 105-mm and 155-mm Projectiles and (b) Average Sensor Altitude Above Each Seed Item (calculated using a 5-m radius centered about each seed location). 17
Figure 6. Number of MARS and Helimag Anomalies as a Function of Amplitude in Areas 1 and 2. 24
Figure 7. Comparison of MARS and HeliMag Densities in Area 1: (a) MARS Total Gradient Image, (b) HeliMag Total Gradient Image, (c) MARS Target Density with 4 nT/m Threshold, (d) HeliMag Target Density with 3 nT/m Threshold, and (e) MARS Target Density with 3 nT/m Threshold. 26
Figure 8. Comparison of MARS and HeliMag Densities in Area 2: (a) MARS Total Gradient Image, (b) HeliMag Total Gradient Image, (c) MARS Target Density with 2 nT/m Threshold, (d) MARS Target Density with 3.8 nT/m Threshold, and (e) HeliMag Target Density with 3 nT/m Threshold. 27
Figure 9. Point-By-Point Comparison of MARS and HeliMag Anomaly Densities in Area 1 and Area 2, Using Two Different Target Thresholds for the MARS Data. 28
Figure 10. Comparison of MARS and HeliMag Sensor Elevations in Area 2. 28
Figure 11. ROC Curves for the MARS and HeliMag Using the Ground-Based Data as Truth. 30
Figure 12. KPBR MARS Survey Southern Area Total-Field Anomaly Map with Manually Selected Targets Overlain. B-1
Figure 13. KPBR MARS Survey Northern Area Total-Field Anomaly Map with Manually Selected Targets Overlain. B-2
Figure 14. Map Showing the Location of the Two Areas Selected for Comparison of the MARS, HeliMag, and Ground-Based Datasets. B-3
Figure 15. Total-Field Data from a Previous HeliMag Survey of the Northern Part of the KPBR Site with Manually Selected HeliMag Anomalies Overlain. B-4
Figure 16. Comparison of (a) Ground-Based, (b) Upward Continued Ground-Based (2 m), (c) MARS, and (d) HeliMag Data on Grid 1a. B-5

LIST OF TABLES

Page

Table 1. MARS Technology Components 3
Table 2. MARS Survey Sites. 6
Table 3. Heading Effects and Noise Levels from High Altitude Test Flights in December 2006 and May 2007. 6
Table 4. Performance Objectives for the MARS Demonstration. 9
Table 5. Bias and Standard Deviations of Daily Calibration Variables 16
Table 6. Detection Results for Seeded Ground-Truth Items (as scored by IDA). 17
Table 7. Performance Criteria. 22
Table 8. Expected Performance and the Confirmation Methods Employed 23
Table 9. Cost Tracking. 31
Table 10. MARS-HeliMag Cost Comparison. 34
Table 11. MARS-HeliMag Cost Comparison Summary. 35

ACRONYMS AND ABBREVIATIONS

3-D	three-dimensional
AGL	above ground level
AVR	Advanced Visual RISC
cm	centimeter
CSM	Conceptual Site Model
DAS	data acquisition system
DEM	Digital Elevation Model
DGM	digital geophysical mapping
DoD	Department of Defense
DOP	dilution of precision
ESTCP	Environmental Security Technology Certification Program
FAA	Federal Aviation Administration
FUDS	Formerly Used Defense Sites
GIS	Geographic Information Systems
GPS	Global Positioning System
HAE	height above ellipsoid
HEAT	high-explosive anti-tank
HeliMag	helicopter magnetometry
Hz	Hertz
IDA	Institute of Defense Analysis
IPR	In-Progress Review
KPBR	Kirtland Precision Bombing Range
LiDAR	light detection and ranging
LSA	light sport aircraft
m	meter
MARS	Minimum Altitude Remote Sensing
MEC	munitions and explosives of concern
MTADS	Multi-Towed Array Detection System
NDIA	New Demolitions Impact Area
NMEA GGK	National Marine Electronics Association time, position, position type, and DOP designation
nT	nanotesla

Pd	probability of detection
Pfa	probability of false alarm
PPS	pulse-per-second
RISC	Reduced Instruction Set Computer
ROC	receiver operating characteristic
RTK	real-time kinematic
SKY	Sky Research, Inc.
SORT	simulated oil refinery target
SW	Short Wing
UTM	Universal Transmercator
UXO	unexploded ordnance
WAA	wide area assessment

ACKNOWLEDGEMENTS

This Cost and Performance Report for the Multi-Sensor Fixed Wing Airborne System MARS, documents the analysis of the MARS system performance and acquisition, processing, analysis, and interpretation of the MARS system magnetometry data collected to demonstrate this technology for detecting unexploded ordnance at the former Kirtland Precision Bombing Range. The work was performed by Sky Research, Inc. of Oregon, with Dr. Stephen Billings serving as Principal Investigator and Mr. David Wright serving as Co-Principal Investigator. Mr. Edgar Schwab of SeaTerra GmbH, Germany, was a research partner and the original technology developer.

Funding for this project was provided by the Environmental Security Technology Certification Program Office. This project offered the opportunity to demonstrate this technology and evaluate its potential use to support the Department of Defense's efforts in efficiently characterizing large Department of Defense sites.

We wish to express our sincere appreciation to Dr. Jeffrey Marqusee, Dr. Anne Andrews, and Ms. Katherine Kaye of the ESTCP Program Office for providing support and funding for this project. We also would like to acknowledge the support and direction provided by Mr. Scott Millhouse of the Huntsville USACE, the COR for this project.

We also would like to acknowledge and express our appreciation for the support of David Henry and David Holladay of the Albuquerque Branch of the USACE for the time spent providing site background information and coordinating access, Steve Abieta and Mark Dixon of the Pueblo of Isleta Environment Department, and the City of Albuquerque Police and Bernalillo County Sheriff department's range masters for coordinating survey access for the shooting range.

Technical material contained in this report has been approved for public release.

This page left blank intentionally.

1.0 EXECUTIVE SUMMARY

The objective of this project was to demonstrate and certify a fixed-wing platform for low-cost, high-resolution wide area assessment (WAA) of former and active military facilities contaminated with unexploded ordnance (UXO). The Minimum Altitude Remote Sensing (MARS) airborne UXO mapping system was developed, successfully tested, and deployed in Europe by SeaTerra GmbH in Germany. The principal objectives of this demonstration were to test and evaluate the MARS system in the United States and compare the performance, results, and cost to HeliMag technology. The site selected for demonstration was the Former Kirtland Precision Bombing Range (KPBR), located near Albuquerque, New Mexico.

Sky Research, Inc. (SKY) acquired the CT Short Wing (SW) model light sport aircraft (LSA) for this demonstration. This model lightweight aircraft, a slightly different model than the one used by SeaTerra in Europe, did not affect the deployment of the technology. The aircraft has an 8.9 m wingspan, a length of 6.2 m, and can fly at a minimum height above ground of 2 m. It uses modern German glider structural design techniques and is essentially all-composite glass fiber reinforced plastic with very little ferrous metal and a low signature footprint. An array of six Geometrics Model 822A cesium vapor magnetometer sensors was mounted on a sensor boom attached to the aircraft wings. The sensors were deployed at separations between 1.15 and 2.0 m. SeaTerra's AGS MK3 frequency counter and data acquisition system (DAS) were used to record data at between 140 to 160 Hertz (Hz) with a ~0.2 nanotesla (nT) noise floor on the outer sensors and 0.5-0.7 nT noise floor on the inner sensors (after processing).

Daily flight durations were planned to be approximately 6 hours per day (assuming an 8-hour daily window for flying). Because of unfavorable weather conditions (frequent high winds and rain or thunderstorms), density altitude[1], and thermal effects that were encountered, it was not possible to safely operate the CT as many hours per day as planned. Daily flight durations ranged from 1.4 hours to a maximum of 5.2 hours, with an average of 3.5 hours for days when conditions for flying were favorable. There were 3 days that no flights were conducted due to rain and/or high winds. During the survey, data were collected over 2,856 acres.

A number of 105-mm high-explosive anti-tank (HEAT) 105-mm and 155-mm projectiles were blind-seeded in an area south of the Double Eagle Airport. For manually selected target picks, there were 2.1 anomalies per acre, and detection probabilities were 11, 60, and 93% for the 105-mm HEAT, 105-mm projectile, and 155-mm projectile, respectively. Using an automatic detection algorithm and a threshold of 5 nT, anticipated detection probabilities were 62, 71 and 100% for the above three items with 19 alarms per acre.

A HeliMag survey was flown over the survey area in 2005, and portions of the site were also covered by a towed-array survey. When target picking using the total-gradient data, the MARS system experienced an inflection point at around 4 nT/m (where the number of alarms increases markedly), compared to 3 nT/m for the HeliMag data.

[1] This is the altitude in the International Standard Atmosphere at which the air density would be equal to the actual air density at the place of observation.

We compared the MARS and HeliMag anomaly density maps in two regions of the northern part of the site (Areas 1 and 2). In Area 1, the MARS and HeliMag derived densities were comparable, and both predicted a target of approximately the same size, shape, and concentration. In Area 2, the density estimates were considerably different with the MARS densities—on average, 3.5 times lower than the HeliMag. This difference was largely attributed to the approximately 1.0 m higher elevation of the MARS sensors compared to the HeliMag. The differences were particularly marked around a fence that cut across a high concentration target region. The CT aircraft had to fly higher over the obstacle and took longer to return to its normal survey altitude than the helicopter.

Using the towed-array data as groundtruth, the HeliMag system exhibited detection probabilities (Pd) of Pd=0.9 on Areas 1 and 2 at five false-alarms per acre. In contrast, for Area 1 the MARS Pd=0.7 at five alarms per acre and rose slowly to Pd=0.85 at 30 alarms per acre. MARS detection performance was significantly worse for Area 2, with Pd=0.6 at around five false alarms per acre, rising to Pd=0.8 at 20 false alarms per acre.

The pilots were able to consistently fly the aircraft at the target 2 to 3 m above ground level. However, the poor detection performance in Area 2, especially in the area where the pilot had to avoid a fence, indicates that surface tracking is more problematic for the CT than a helicopter.

The main difference in cost between MARS and HeliMag is in the cost of the aircraft, with daily helicopter costs approximately five times that of MARS. Depending on the distance required for mobilization and the size of the area surveyed, a MARS survey costs 51 to 66% of a HeliMag survey. For large sites (10,000 acres) with small mobilization distances (< 4 hours), MARS would cost about $55 per acre. For smaller sites (1,000 acres) and greater mobilization distances (> 16 hours), MARS would cost approximately $134 per acre.

2.0 INTRODUCTION

2.1 BACKGROUND

This project was conducted to demonstrate and certify a fixed-wing platform for deploying low altitude remote sensing technologies that can be used to help meet the increasing demand on the Department of Defense (DoD) for low-cost, high-resolution wide area assessment (WAA) of former and active military facilities contaminated with unexploded ordnance (UXO). The objective of the demonstration of the Minimum Altitude Remote Sensing (MARS) system is to evaluate the ability of this platform and technology to characterize large sites cost efficiently, reliably, and safely. The MARS airborne UXO mapping system was developed, successfully tested, and deployed in Europe by SeaTerra GmbH in Germany. Sky Research, Inc. (SKY) is demonstrating and certifying this system (Figure 1) for application in the United States in partnership with SeaTerra.

The site selected for demonstration is the Former Kirtland Precision Bombing Range (KPBR) located near Albuquerque, New Mexico, in order to provide the ability to compare performance, results, and cost with another low altitude WAA technology, helicopter magnetometry (HeliMag). HeliMag was previously demonstrated at the site as part of the Environmental Security Technology Certification Program (ESTCP) WAA Pilot Program. In addition, the results of this demonstration will be integrated into the SKY WAA Geographic Information System (GIS) with the WAA data collected at the site (HeliMag, Light Detection and Ranging [LiDAR], orthophotography, and ground-based digital geophysical mapping [DGM] data) to facilitate data analysis, historical information integration, and data access.

Figure 1. The CT SW Light Sport Aircraft Collecting Data at the Former Kirtland Precision Bombing Range.

2.2 OBJECTIVES OF THE DEMONSTRATION

The principal objectives of the MARS project are to test and evaluate the MARS system in the U.S. and compare the performance, results and cost to HeliMag technology. Similar to HeliMag, MARS is expected to demonstrate efficient, low-altitude DGM capabilities for metal detection at

a resolution approaching that of ground survey methods, limited primarily by terrain, vegetation, and topographic inhibitions to safe low altitude flight.

2.3 REGULATORY DRIVERS

The Former KPBR is a WWII-era former military training facility located approximately 10 miles west of Albuquerque. The site is classified as a Formerly Used Defense Site (FUDS). ESTCP established a 6,500 acre demonstration plan sub-area for the WAA Pilot Program in 2005, and the MARS demonstration survey also was conducted within the WAA boundary. Results from the data analysis for the WAA Pilot Program confirmed the presence of three precision bombing targets (N2, N3, and New Demolitions Impact Area [NDIA]) and a simulated oil refinery target (SORT), and several additional areas of interest. Currently, most of the study area is undeveloped; however, portions of the area are planned for commercial or industrial development within the next decade. The KPBR site also encompasses the Double Eagle Airport, which is owned by the City of Albuquerque. The airport is very active and there are plans for future expansion of aviation facilities and infrastructure, as well as promotion of business development to attract aviation-related businesses. It will be necessary to ensure that any munitions-related contamination is fully characterized and remediated to allow for airport expansion and business development.

3.0 TECHNOLOGY

3.1 TECHNOLOGY DESCRIPTION

The technology components, including the aircraft, and all sensor and positioning components and associated electronics are described in the following sections.

3.1.1 Airborne Platform

SKY acquired the CT Short Wing (SW) model light sport aircraft (LSA) for this demonstration. This model lightweight aircraft, a slightly different model than the one used by SeaTerra in Europe, did not affect the deployment of the technology. The aircraft has an 8.9 m wingspan, a length of 6.2 m, and can fly at a minimum height above ground of 2 m. It uses modern German glider structural design techniques and is essentially all-composite glass fiber reinforced plastic with very little ferrous metal and a low signature footprint. The aircraft serves as the platform for deployment of the sensor and positioning technologies used for this demonstration (Table 1).

Table 1. MARS Technology Components

Technology Component	Specifications
Geophysical sensors	6 Geometrics G-822A cesium vapor magnetometers
Global Positioning System (GPS) equipment	Trimble AgGPS model 132 for navigation and Trimble MS750 system with 2 GPS receivers for precise real-time kinematic (RTK) positioning
Altimeters	1 Reigel laser altimeter
Inertial measurement	SeaTerra compensation system
Magnetic compensation (and redundant attitude information)	SeaTerra digital compass and proprietary magnetic compensation system
Data acquisition system (DAS) and frequency counter	AGS MK3 (SeaTerra proprietary DAS and frequency counter): Better than 0.1 nanoTesla (nT) resolution at, 150 Hz: 0.1 to 0.7 nT noise floor
Aircraft	Flight Designs CT SW

3.1.2 Airborne Sensors and Boom

An array of six Geometrics Model 822A cesium vapor magnetometer sensors are mounted on the sensor boom (Figure 2). The sensor system is mounted on the CT SW with support structures fixed to the aircraft wings. We attempted to maintain consistent 1.4-m spacing between sensors but found that we could achieve much lower noise levels if we moved several of the sensors. In particular, the two inner sensors (numbers 3 and 4) were moved so they were 2.0 m apart, with the other sensors between 1.15 and 1.4 m apart. Sensor 2 was moved a little closer to sensor 1 to place it further from the laser altimeter which appeared to be causing a small increase in the noise level of that sensor.

SeaTerra's AGS MK3 frequency counter and DAS were used to record data at around 160 Hz with a ~0.2 nT noise floor[2] after processing.

[2] The inner sensors 3 and 4 exhibited noise levels between 0.45 and 0.7 nT.

This system was thoroughly tested on the MARS platform during field trials and production work within Germany. As part of this project, the aircraft modifications were required to be approved for deployment in the United States. Consultation with the Federal Aviation Administration (FAA) resulted in direction to obtain the manufacturer's approval of the modifications. Because the CT falls in the LSA category, the FAA does not have any requirements or authority to approve modifications. SKY provided the specifications and engineering drawings for the sensor boom and other components to the Ukrainian manufacturer for their evaluation and testing to obtain the required approvals.

3.1.3 Positioning Technologies

For the demonstration survey, we also deployed two Trimble MS750 GPS units configured in a Moving Base–Rover mode to provide National Marine Electronics Association GGK (NMEA time, position, position type, and dilution of precision [DOP] designation) positions at 20 Hz GPS and Advanced Visual RISC [Reduced Instruction Set Computer] (AVR) orientation data at 10 Hz (this is the same system used successfully for the HeliMag technology). The system requires two MS750 Marine GPS receivers, two compact L1/L2 GPS antennas, 12-24 Volt power, and RTK corrections. The GPS antennas were flush-mounted close to the wing tips on both sides of the aircraft, in line with the magnetometer boom. This provided a baseline of 6 m. The NMEA GPS data provide the latitude and longitude of antennas while the AVR data return the platform roll and yaw (an equivalent concept is used very successfully in the HeliMag system).

A Reigal laser altimeter recorded the aircraft height above ground at cm-level accuracy at a sample rate of 50 Hz. Since the fixed-wing system does not change altitude quickly, the altitude values show nominal variation, and the normal flight height above ground is 2-3 m. The 3-D position of each data point was utilized in subsequent processing (e.g., the magnetic inversion modules in UXOLab allow inversion of magnetic data with variable altitudes).

3.1.4 Development and Prior Testing of the Technology

SeaTerra GmbH, partnered with SKY for this project, developed and has deployed the MARS system. The system was used to survey nearly 8,000 survey acres at sites in Europe prior to initiating this project. Adaptation of the sensor boom for the CT SW and certification of the system for use in the United States were conducted from May to November, 2006. Pre-demonstration test flights were conducted in December, 2006 and April, 2007 to confirm that the system was operating within specifications.

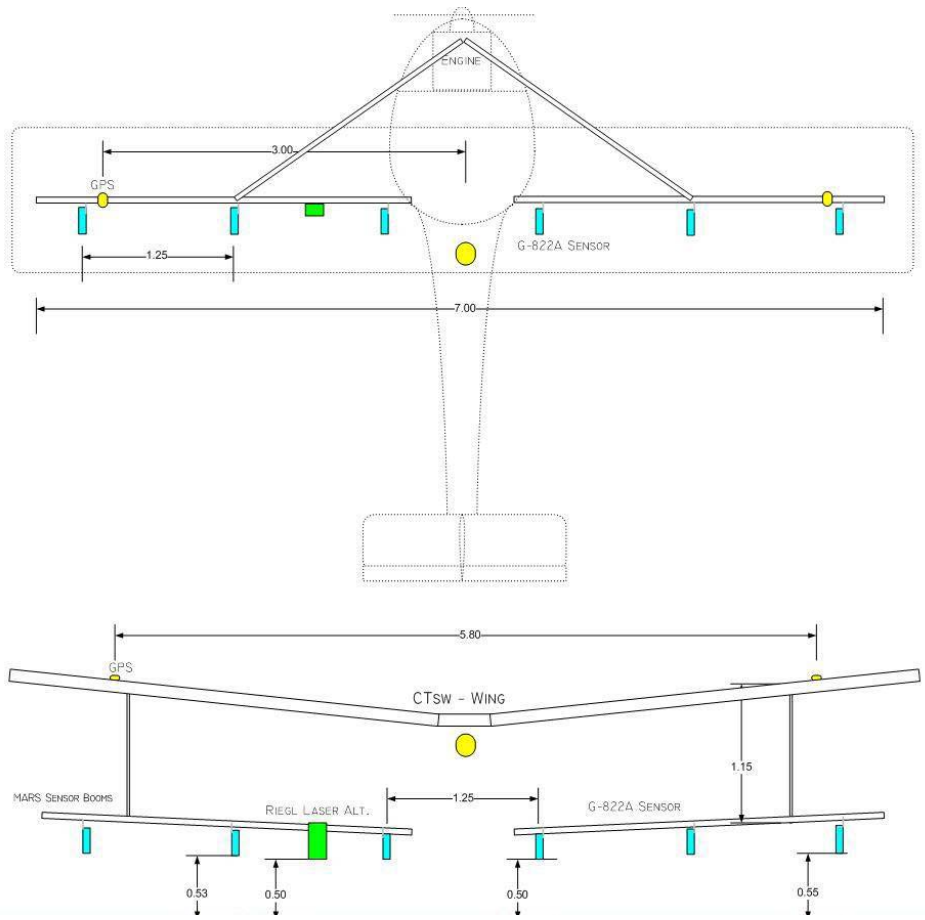

Figure 2. Schematic of the MARS Sensor Layout.
(In this diagram the sensors are shown 1.25 m apart. For this demonstration, we used a sensor spacing of between 1.1 and 2.0 m.)

The MARS system was tested by the German government on military ranges in southern Germany. In addition, it was used to conduct four commercial WAA UXO surveys covering nearly 8,000 acres in Germany between 2001 and 2006. A summary of the previous application of the technology to munitions and explosives of concern (MEC) site characterization is provided in Table 2. Achieved productivity on these sites ranged from 250-500 acres/day. The system proved to be very accurate, efficient, reliable, and suitable even in areas that were considered non-ideal. The statistical approach of calculating relative density distribution coefficients has proven to be reliable, and the results correlate with ground truth surveys and excavations. Since an array of cesium vapor magnetometers are the main detection sensors, the ability to detect small ferrous objects is diminished as the separation between the sensor and the target increases. However, at 2 m elevation, MARS is capable of detecting 2.75-inch rockets and larger items of interest.

Table 2. MARS Survey Sites.

German Training Range	Oversight	Total Area (acres)	Survey Area (acres)	Vegetation Condition	Topo-graphic Relief	Facility Use
Műnsingen	Government	16,055	3,952	40% wooded	250 m	150 years: Artillery, infantry,tank training, bombing
Eggersdorf	Private investor	6,175	988	Free	0 m	100 years: Military airfield
Oranienburg	Government	2,470	494	50% wooded	2 m	100 years: Air Force Base
Trampe	Germany – EPA	14,820	1,976	30% wooded	30 m	50 years: Tank training

Development of the system was conducted under this project to fabricate and certify a sensor boom that could be mounted to the CT SW. Because of the structural differences between the SW and German-based CT, an engineering analysis was required to select the appropriate mounting locations on the wings and design the sensor boom struts. The design was conducted in conjunction with the Ukrainian manufacturer, and certification of the modified boom design was granted upon successful structural and weight tests.

Table 3 summarizes the results of a final high-altitude characterization test with the system configured and ready for the demonstration. A 20-second segment of the flight, with the aircraft flying straight, was used to characterize the sensor noise levels. The noise levels (after processing) in sensors 3 and 4 were reduced by a little less than half of the values found during test flights conducted in December 2006. The values for sensors 1, 2, 4, and 6 were between 0.14 and 0.19 nT. All values were less than our demonstration objective of less than 1 nT.

Moving the inner sensors slightly further apart (as well as replacing the ferrous bolts on the wheels) significantly reduced the effects of heading on the magnetic field recorded by these sensors (Table 3). During the execution of a turn (that was very similar to the turn analyzed in December 2006), sensors 3 and 4 showed less variation relative to sensor 1 than the previous test and had a lower bias compared to that previous test (potentially due to the removal of the permanent magnetic field caused by the bolts on the wheel).

Table 3. Heading Effects and Noise Levels from High Altitude Test Flights in December 2006 and May 2007.

Sensor	Maximum difference (nT) relative to sensor 1 (during turn)		Standard deviation (nT) (straight line segment)	
	Dec 06	May 07	Dec 06	May 07
Sensor 1	0.0	0.0	0.10	0.16
Sensor 2	175	212	0.23	0.14
Sensor 3	1270	489	1.19	0.67
Sensor 4	883	359	0.73	0.45
Sensor 5	162	195	0.29	0.19
Sensor 6	175	167	0.22	0.13

3.2 ADVANTAGES AND LIMITATIONS OF THE TECHNOLOGIES

As with all characterization technologies, site specific advantages and disadvantages exist that dictate the level of success of their application. The general advantages of MARS technology include:

- The ability to characterize very large areas
- Lower cost as compared to ground-based and helicopter-based DGM methods.

Because of the lower costs associated with the aircraft maintenance and acquisition costs and much lower fuel consumption, the MARS system is expected to demonstrate a much lower cost to operate than HeliMag.

There are advantages and disadvantages in using a fixed-wing platform. Open areas are very suitable for the fixed-wing systems. MARS can be flown quite flexibly, but obstacles such as trees and power lines pose a safety hazard and have to be flown over, producing data gaps. In these conditions the helicopter platform, the primary alternative technology, will outperform MARS. The topography of a survey site plays a role as well. If the area is slightly hilly, MARS has no deployment limitations. However, mountainous areas and steep slopes are not suitable for fixed-wing systems. An advantage of MARS is the ability to fly more constant flight paths and straighter survey lines. An advantage of the fixed-wing platform is that rapid positioning changes (change of direction and speed) do not occur frequently, and therefore problems in positioning are generally avoided.

For all airborne surveys, the largest single factor affecting the survey costs is the cost of operating the survey aircraft and sensors at the site. These equipment costs are related to capital value, maintenance, overhead, and direct operating costs of the sensor and aircraft systems. Mobilization to and from the site increases costs as distance traveled increases, and flexibility of scheduling is critical in determining whether mobilization and deployment costs can be shared across projects. In addition, low altitude surveys are limited by topography and vegetation and therefore airborne technologies can be deployed only to sites with suitable conditions.

An advantage of the MARS system is the low-noise aspect of this platform. The CT SW aircraft is made entirely of fiberglass composite materials; the only major metallic component is the engine. Since the rotation of the engine is very high-speed, it only creates a high frequency noise to the data, which is above the frequency of the signal from items of interest in the ground. Most of the fixed metallic components of the system were replaced by nonmagnetic components. The remaining metal parts are the engine and the rescue system of the plane, which are both fixed and create a constant signature depending on the movement of the plane in the magnetic field. This heading dependent signature can be removed with the use of appropriate high-pass filters. Careful attention has been given to the relative timing of the different sensors in the MARS system to avoid time delays or synchronization problems. Calibration loops flown in high altitude provide estimates of plane noise in correlation with the plane movement and orientation. Typical noise levels during operation are ~0.3 nT. This is the noise in the raw data, which fortunately has a very high frequency. A frequency domain filter is applied to produce data in the 0.1 to 0.2 nT range[3]. These are comparable to noise levels achieved in the HeliMag systems. For

[3] For the inner sensors we could only achieve noise floors between 0.5 and 0.7 nT.

instance, our analysis of the Hughes 500 helicopter as part of the ESTCP MM0535 deployment to Toussaint River revealed noise levels of 0.07 to 0.11 nT.

An additional consideration for the MARS system is the window for safe flying conditions for a fixed-wing aircraft. Several additional factors more significantly affect safe operation of a lightweight, fixed-wing aircraft compared to a helicopter. These include:

- Windspeeds less than approximately 15 mph (~13 knots) are considered safe and allow the pilot to maintain planned flight lines without major deviations.

- Ground effects, caused by the reduction of induced drag when an airplane is flown at slow speed very near the ground surface can present a hazard. Ground effect exerts an influence only when the airplane is flown at an altitude no greater than its wing span. The effect increases as the aircraft descends closer to the ground, with the most significant effects occurring at a height of one-half the wingspan above the ground. It can present a hazard for low-level flight because the varying drag must be corrected for as the aircraft changes altitude to adjust to varying terrain, obstacles, or for other reasons, and there is little room for error in making adjustments at such low altitudes. The optimal survey altitude falls within this range.

- Density altitude is defined as the pressure altitude corrected for nonstandard temperature variations. A simple definition of density altitude is "the altitude the airplane thinks it is at, and performs in accordance with." High density altitude can significantly affect flight characteristics, reducing the lift and power output of the aircraft and limiting safe flight operations, particularly for low-level flight. Both altitude and temperature affect the density altitude. The KPBR site is at around 5,800 feet in elevation (1,770 meters).

The ground effects and density altitude issues also affect helicopter operation but less significantly than the fixed-wing aircraft. This has the result of more limited flight time due to site altitude and weather conditions and has the potential to offset the advantage of lower operational costs to some degree.

4.0 PERFORMANCE OBJECTIVES

Performance objectives are a critical component of this demonstration because they provide the basis for evaluating the performance and costs of the technology. For the MARS project, both primary and secondary performance objectives were established. Table 4 lists the performance objectives for the MARS technology, along with criteria and metrics for evaluation. Many of the performance objectives have been developed to parallel those for the HeliMag system since an important component of this demonstration is to compare the performance of the MARS to that system.

ESTCP emplaced test items at the Former KPBR site to be used as a blind test to validate the system's performance. Scoring of these items is one of the primary metrics for evaluating the MARS system performance.

Table 4. Performance Objectives for the MARS Demonstration.

Type of Performance Objective	Primary Performance Criteria	Expected Performance (Metric)	Actual Performance Objective Met?
Primary/ Qualitative	Ease of use and efficiency of operations for sensor system	Efficiency and relative ease of use	No
Primary/ Quantitative	Geo-reference position accuracy	Within 0.5 m (determined by ESTCP and daily calibration target dipole fit position estimates)	No
	Target feature definition	Bias and standard deviation of daily calibration target dipole fit parameters within 25% of values for previous Kirtland HeliMag deployment	Yes
Primary/ Quantitative	Probability of detection (Pd) relative to the HeliMag	Pd (MARS) > 0.9 Pd (HeliMag) Pfa(MARS) < 0.5 (based on comparison with vehicular)	No
Primary/ Quantitative	Detection probability on emplaced objects	Pd (MARS) > 0.9 for items of 105-mm caliber and greater	No
Secondary/ Quantitative	Terrain/ vegetation/infrastructure restrictions	Acres surveyed with MARS > 90% of planned survey area	No
Secondary/ Quantitative	Operating parameters (altitude, speed, production level)	2-3 m above ground level (AGL); 68 knots (35 m/s); 400 acres/day	Yes
Secondary/ Quantitative	Ease of use: Navigational accuracy	95% of actual flight path within 2 m of planned flight path	NA
Secondary/ Quantitative	Noise level (combined sensor/platform sources, post-filtering)	< 1 nT on all sensors determined by high altitude test flights	Yes
Secondary/ Quantitative	Data density/point spacing	< 0.175 m along track < 2 m cross track	No

This page left blank intentionally.

5.0 SITE DESCRIPTION

5.1 SITE LOCATION AND HISTORY

The Former KPBR is a WWII-era former military training facility located about 10 miles west of Albuquerque, New Mexico. This FUDS consists of a total of ~38,000 acres, encompassing multiple target areas. It served as a training area for Kirtland Air Force Base during WWII. WAA demonstrations were conducted on the 5,000 acre demonstration site located on either side of Double Eagle Airport. The physiography and known munitions-use history of the study area are discussed in detail in the Conceptual Site Model (CSM) (Versar, 2005).

The study area was known to contain three precision bombing targets identified as N-2, N-3, and NDIA, as well as a SORT. The CSM did not indicate any munitions-related activity in the southern portion of the study area. Figure 3 shows the MARS survey area within the WAA study area, along with infrastructure and other site features.

5.2 SITE GEOLOGY

The study area is on a relatively flat terrace at about 6,000 feet elevation (mean sea level) atop the Rio Puerco Escarpment, which falls away to the west of the site. To the east of the study area, several volcanic cinder cones rise about 300 ft above the surrounding terrain. The soils within the survey area are deep, well-drained homogeneous sandy loams formed on loess parent material with low magnetic mineral content.

5.3 MUNITIONS CONTAMINATION

Documented ordnance present on the site surface within the study area includes the following: (1) M38A2 100-lb practice bombs and spotting charges; (2) M85 100-lb practice bombs and spotting charges; and (3) 250-lb general purpose HE bombs.

5.4 PRE-DEMONSTRATION TESTING AND ANALYSIS

Previous testing and analysis has been performed at the Former KPBR site under the existing ESTCP WAA Pilot Program. HeliMag (performed by SKY), LiDAR, and very large scale orthophotography (performed by other demonstrators) data were collected over the same area surveyed using the MARS technology. The results of the previous analyses confirmed the presence of target areas identified in the CSM, and several additional areas of concern were identified based on features and anomaly densities identified in the WAA analysis. Because both HeliMag and MARS technologies collect data using magnetic sensors, comparison of the two datasets provides a cross-check of both technologies.

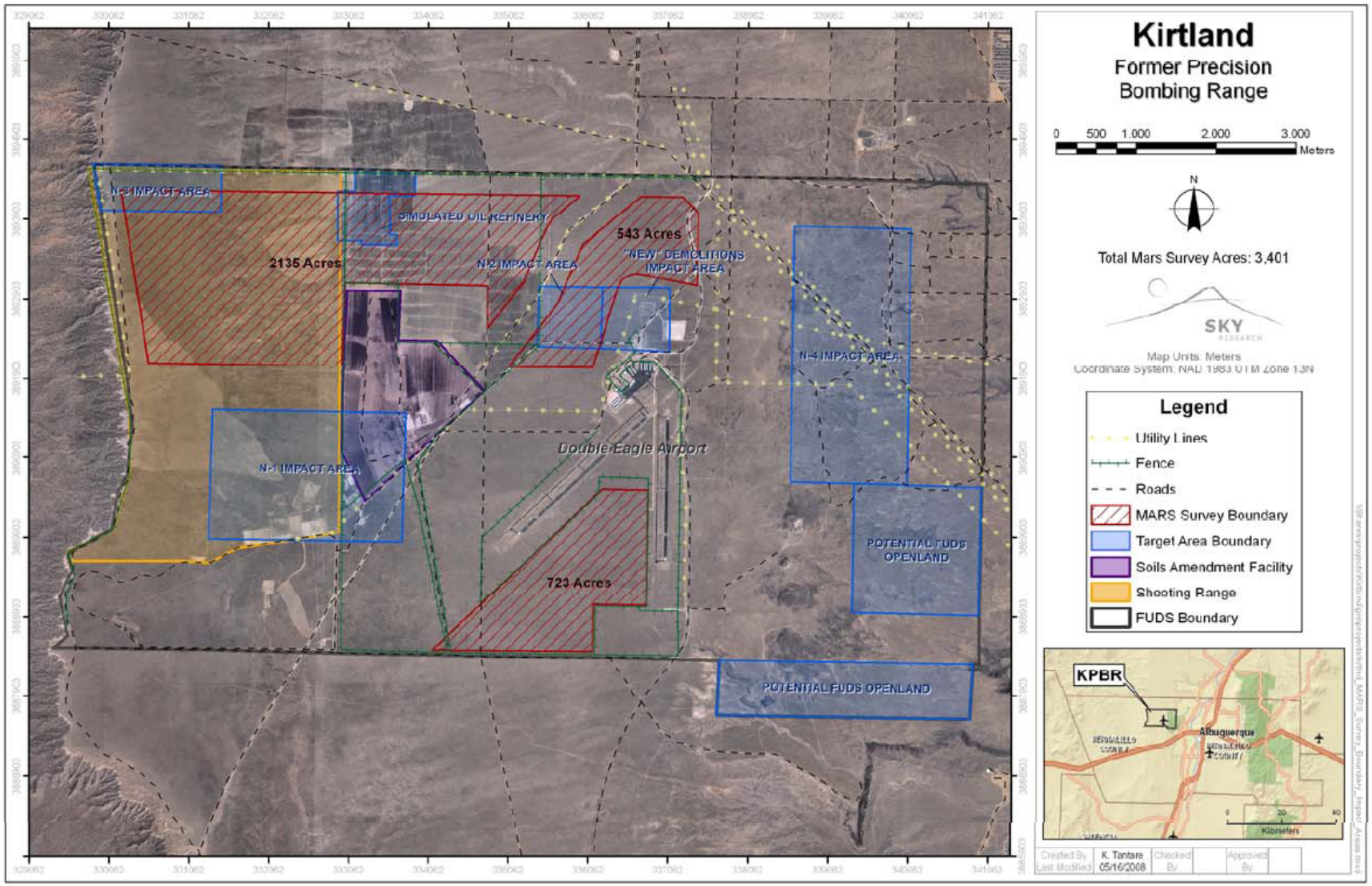

Figure 3. Former Kirtland Precision Bombing Range with Identified Bombing Targets and other Areas of Interest, Including Existing Features and the Utilities Infrastructure.
(Note that the power line that splits the northern area in two was actually buried, so that it was possible to survey that "buffer zone.")

6.0 TEST DESIGN

The MARS system survey was designed to demonstrate the system in the United States and assess the performance and capabilities relative to HeliMag technology. Because both HeliMag and MARS technologies collect data using magnetic sensors, comparison of the two datasets provides a cross-check of both technologies. Previous testing and analysis have been performed at the Former KPBR site under the existing ESTCP WAA Pilot Program. HeliMag (performed by SKY), LiDAR, and very large scale orthophotography (performed by other demonstrators) data were collected over the same area surveyed using the MARS technology. The results of the previous analyses confirmed the presence of target areas identified in the CSM, and several additional areas of concern were identified based on features and anomaly densities identified in the WAA analysis.

6.1 CONCEPTUAL EXPERIMENTAL DESIGN

The scope of the survey planned at the Former KPBR included the three confirmed target areas and the simulated oil refinery target (Figure 3). This area coincides with the area previously surveyed using the HeliMag technology to provide a direct comparison of the magnetic data collected using the two different platforms. A portion of the 5,000 acres flown by the HeliMag system was inaccessible because of infrastructure present at the site (high voltage power lines, etc.); however, data were collected over as much of the area as could be safely flown. Additionally, test items were blind-seeded at KPBR and the results used as one of the primary criteria for evaluating the MARS system's detection capabilities.

6.2 SITE PREPARATION

Because the KPBR site is a WAA site and had been previously surveyed, the only site preparation needed for the MARS demonstration was the emplacement of test items and setup of the calibration line. The field deployment schedule was coordinated with the Program Office schedule for emplacing the test items in the areas of the site north and south of the Double Eagle airport. Battelle was conducting a demonstration of another system concurrent with the MARS test, so setup of the calibration lines was coordinated with their site team. No other physical site preparation was needed prior to conducting the survey.

6.3 SYSTEM SPECIFICATION

The MARS system was deployed on the CT SW LSA, together with a pilot and a two- to three-person ground support team to operate the RTK GPS base stations, download data, refuel the aircraft, etc. The system used an array of six total-field cesium vapor magnetometers deployed on a 7-m boom mounted under the aircraft wings. The planned aircraft altitude was 2-5 m, with an average forward velocity of 35 m per second (m/s).

6.4 DATA COLLECTION

The demonstration survey was conducted between April 24th and May 8th, 2007. Daily flight durations were planned to be approximately 6 hours per day (assuming an 8-hour daily window for flying). Because of unfavorable weather conditions (frequent high winds and rain

or thunderstorms), density altitude[4], and thermal effects that were encountered, it was not possible to safely operate the CT as many hours per day as planned. Daily flight durations ranged from 1.4 hours to a maximum of 5.2 hours, with an average of 3.5 hours for days when conditions for flying were favorable. There were 3 days when no flights were conducted due to rain and/or high winds. After approximately a week into the field deployment, it was apparent that surveying the planned 5,000 acres would not be feasible within the projected schedule and project budget but that sufficient data were being collected to assess the technology. Therefore, upon discussion and with direction from the Program Office, the survey was truncated after 2 weeks of survey flights, as presented in the demonstration plan.

During the survey, data were collected over 2,856 acres. This comprised approximately 700 acres south of the Double Eagle Airport at KPBR (Figure 12 [Figures 12-16 are included in Appendix B]) and 1,400 acres north of the airport (Figure 13). The additional 650 acres were split between the Shooting Range area in the western part of the site (Figure 13), where coverage was patchy (400 acres), and re-flights to remedy data quality problems.

The truncation of the survey meant that there was no time to fill in the gaps in coverage in most of the southern and northern sections of the KPBR site. The result was that there were a number of long, thin gaps in survey coverage (Figures 13 and 14). Part of the intended survey area in the southern part of the site could not be surveyed due to an FAA exclusion policy regarding overflights of a populated building (the building was just south of the area shown on the map in Figure 12).

We had intended to survey the Shooting Range area on the western side of the map area shown in Figure 13. However, we could access that portion of the site only on certain Mondays and Tuesdays and before 9 A.M. on other days. From the map in Figure 13 it is evident that certain flights extended into the Shooting Range area, while others had to terminate just to the east of the Range. Also evident in Figure 13 is a gap in the coverage just north of the Double Eagle Airport. This corresponded to a zone where we had to carefully schedule our flight activities with Battelle. We had to terminate the survey before we had the chance to complete data collection over that part of the site.

Quality Checks and Sensor Calibration Targets

A calibration line was established near the base of field operations just north of Double Eagle airport. The calibration targets were placed on the ground surface at a spacing of approximately 50 m. The locations of all calibration items were surveyed to verify positional accuracy. A dipole model was fit to the data around each calibration item, and the location and dipole parameters were used to confirm that the system was operating correctly. No calibration targets were buried, and no attempt was made to measure a probability of detection from the calibration data.

The sensor data were passed through a hardware-based 60-Hz noise rejection filter before they were time-stamped. The filter delay is fixed and predictable but we found that we needed to

[4] This is the altitude in the International Standard Atmosphere at which the air density would be equal to the actual air density at the place of observation.

make small adjustments (on the order of 0.01 to 0.02 seconds) to the delay to obtain the best match with the daily calibration data.

The difference in the estimated and actual positions of each calibration item for each calibration run is summarized in Figure 4. The north-south oriented 2.75-inch rocket had too small a signal to be reliably inverted, so it was excluded from the analysis. The estimated positions have a mean bias of 8.6 cm east and 10.7 cm north relative to the true positions (Figure 4a). Approximately 90% of the time, the estimated position was within 50 cm of the actual position (Figure 4b). The predicted dipole depths vary by about 50-60 cm for each item, with no bias for items 1 to 3, a negative bias for item 4 and positive biases for items 5 and 7 (Figure 4c). Finally, Figure 4d shows that the recovered dipole moments are reasonably well clustered, with the largest variance exhibited by the 2.75-inch rocket. This shows that the system performance was comparable on different days.

6.5 VALIDATION

The Program Office arranged for the emplacement of a number of rounds in the southern part of the KPBR survey area. This included eighteen 81-mm mortars, thirteen 105-mm high-explosive anti-tank (HEAT) rounds, seven 105-mm projectiles and twenty-three 155-mm projectiles. In August, we submitted a dig-list with 1,270 anomalies to the Institute of Defense Analysis (IDA) and they calculated detection probabilities based on a 1.5-m detection halo (Table 6). Probabilities of detection ranged from 6% for the 81-mm mortars up to 61% for the 155-mm projectiles. As mentioned earlier, we experienced a glitch in the processing of two flights and hence thought we had two gaps in the data coverage so that no data were collected over 24 of the items. When these items are removed from the analysis, the results for the 81-mm and 105-mm rounds do not change appreciably, whereas the detection probabilities for the 105-mm and 155-mm projectiles increase substantially (to 60 and 93%, respectively).

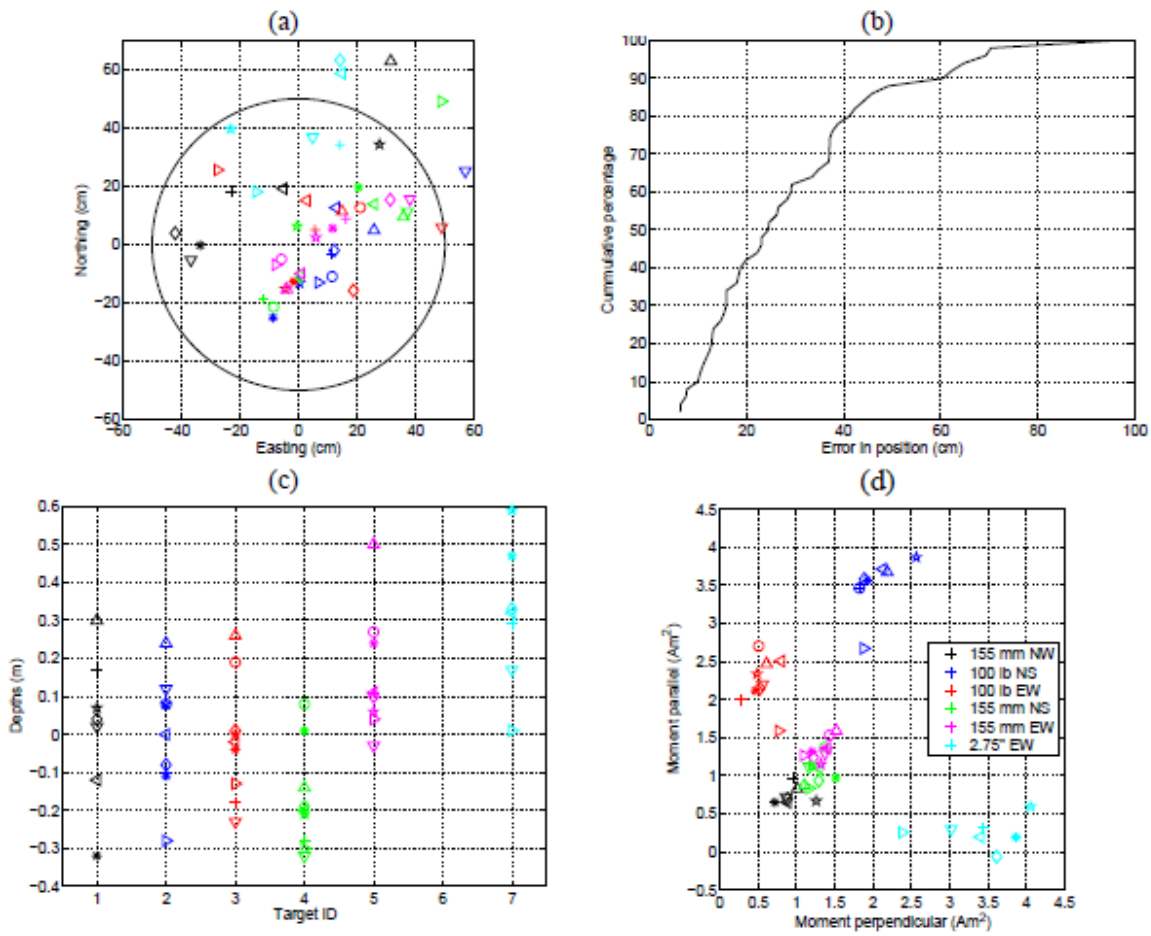

Figure 4. Results of Daily Calibrations (with different days plotted as different symbols, and each calibration item as a different color).
(The blue triangles, stars, and crosses represented calibration results for the N-S oriented 100-lb bomb on different days: (a) positional offset of dipole model fit, (b) cumulative distribution of position errors, (c) estimated depth of calibration items, and (d) recovered dipole moments.)

Table 5. Bias and Standard Deviations of Daily Calibration Variables.
Also shown for reference are the bias and standard deviation of the calibration parameters for the Sky Helimag system (which was deployed at the same site but with a different set of calibration items).

Dipole Fit Parameter	MARS		HeliMAG	
	Bias	Standard Deviation	Bias	Standard Deviation
Easting	0.09 m	0.23 m	0.02 m	0.09 m
Northing	0.11 m	0.23 m	0.06 m	0.13 m
Depth	0.04 m	0.16 m	0.15 m	0.13 m
Size	n/a	7 mm	n/a	7 mm
Angle relative to Earth's field	n/a	3.9 º	n/a	6.0 º

Most manually selected targets had amplitudes between 5 and 15 nT with very few target picks below 5 nT. The detection results can be understood by computing the best and worst case amplitudes for each ordnance item in Figure 5. The magnetic models for the ordnance items were obtained from the test-stand measurements reported in Billings et al. (2006). When the sensor to target distance exceeds about 2.0 m, the amplitude of the 81-mm mortar is less than 5 nT, even for the most favorable orientation. The 5 nT threshold occurs between 1.8 and 2.8 m for the 105 mm HEAT round (depending on the orientation). For the 105-mm projectile, the threshold is reached at between 2.2 and 3.8 m, and for the 155-mm projectile between 3.2 m to about 4.7 m. These calculations are made assuming the item has no remanent magnetization: this will act to either increase or decrease the maximum detection depth, depending on whether it enhances or reduces the total magnetization of the item.

In Figure 5b, we plot the average ground-clearance above each seeded item and find that the sensors were, on average, between 1.4 and 2.6 m aboveground. For most items, the sensors were between 1.6 and 1.8 m aboveground. Thus, it appears that, in this portion of the site, the survey height of the MARS platform was comparable to that expected for the HeliMag system where we would anticipate the height to vary from 1.5 to 2.0 m above the item (under similar favorable conditions of low vegetation and minimal topography).

Table 6. Detection Results for Seeded Ground-Truth Items (as scored by IDA).

Item	Total	In gap	Missed	Detected	Pd (all)	Pd (nogaps)
81 mm mortar	18	10	7	1	6%	13%
105 mm HEAT	13	4	8	1	8%	11%
105 mm Projectile	7	2	2	3	43%	60%
155 mm Projectile	23	8	1	14	61%	93%

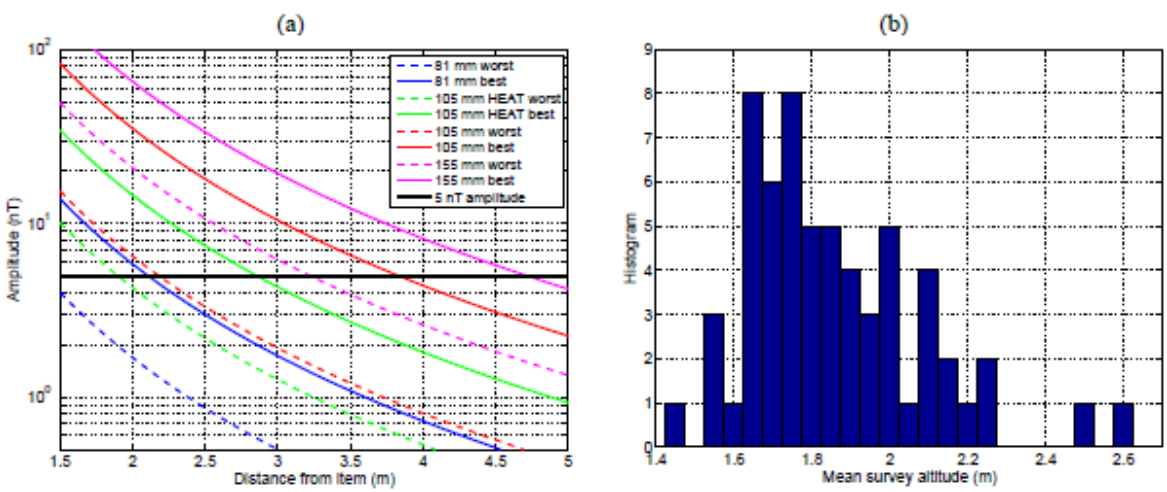

Figure 5. (a) Best and Worst Case Anomaly Amplitudes for the 81-mm Mortar, 105-mm HEAT Round, and the 105-mm and 155-mm Projectiles and (b) Average Sensor Altitude Above Each Seed Item (calculated using a 5-m radius centered about each seed location).

This page left blank intentionally.

7.0 DATA ANALYSIS AND PRODUCTS

7.1 PREPROCESSING

The AG3 MK3 data acquisition system time-stamps each of the sensor readings using an internal clock that is synchronized to the 1 pulse-per-second (PPS) from the GPS. A hardware-based 60 Hz noise rejection filter was used to suppress power-line noise and introduced a fixed delay into the magnetometer data stream. After the survey was completed, the data were processed as follows:

- The raw data for a given survey flight were time-aligned (e.g., the logged GPS times were corrected by reference to the PPS).

- Invalid data were rejected based on status flags present in the raw data records (e.g., poor GPS fix) or, in the case of the magnetometer data, a simple "in range" test was used.

- The GPS geographic position coordinates were transformed to WGS84 Universal Transmercator (UTM) coordinates.

- The GPS, magnetometer, and auxiliary sensor data streams were then merged using the time reference. Using knowledge of the sensor-GPS geometry, each sensor was assigned a position and height above ellipsoid (HAE) based on the UTM location of the GPS receiver, the roll and yaw from the AVR, and the pitch from the digital compass. In practice, we found that the pitch measurements were not reliable and hence were discarded from the processing as described previously.

- To determine the height above ground, one of two methods was used, depending on whether a pre-existing LiDAR dataset was available over the area:
    - LiDAR Digital Elevation Model (DEM) available: The height aboveground was obtained by subtracting the HAE of the LiDAR DEM from the HAE of each sensor.
    - No LiDAR DEM: In that case, the laser altimeter data were used to build a DEM of the area. The DEM was created by using the GPS location and the roll and yaw to determine the position and HAE of the laser reflection. The height aboveground was then obtained by subtracting the HAE of the DEM from the HAE of each sensor.

- The magnetometer data were filtered to remove geological and temporal trends.

- The detrended magnetometer data were gridded at 0.375 m pixel spacing.

In theory, data processing rates should be similar to HeliMag processing, where data collected over 300-500 acres can be processed in less than 4 hours to produce an initial image. In practice, the processing took a little longer because three different software packages were used—SeaTerra's proprietary data processing software, UXOLab, and Geosoft Oasis Montaj. Data were

transferred between each software system using ASCII files, which are time-consuming to read and write.

The initial image was used to check survey coverage and operation of the system. If no problems were detected and the applied filters were appropriate, the image was used for data analysis as described in the section below. If filters were deemed inappropriate, the filter parameters were adjusted and the images recreated.

7.2 TARGET SELECTION FOR DETECTION

Once magnetic anomaly maps were created, anomalies were selected. Automatic target selection for large-scale surveys such as this one has the advantage of being objective and repeatable as well as much faster than manual target selection. Automatic target selection processes have been used for the Former KPBR and the Former Pueblo Precision Bombing Ranges, Colorado, WAA Pilot Program demonstration sites. However, automatic target pickers are not yet sophisticated enough to reliably detect closely spaced targets or targets that are at or below the same amplitude as local geologic signal, and are not able to differentiate between our targets of interest and local geologic anomalies. Therefore, automatic target selection routines must be used only to select targets with response amplitudes significantly above the nominal geologic noise; otherwise, an inordinate number of false targets are selected. Furthermore, the automatic routines do not perform well in areas of high target density. For this demonstration, we manually selected anomalies (except for the performance comparison with HeliMag and ground-based systems where we used automated detection methods in order to be as objective and consistent as possible).

7.3 DATA PRODUCTS

Figures 12 and 13 show the processed total-field images for the southern and northern areas with manually selected targets overlain. The southern area targets were submitted to the Program Office in August 2007 so that the detection performance against seeded targets could be accessed (see Section 8). There were no target picks made in two sections of the site corresponding to the two flights where there was a glitch in processing (see Section 6.5).

8.0 PERFORMANCE CONFIRMATION METHODS

8.1 PERFORMANCE CONFIRMATION METHODS

Table 7 summarizes the performance confirmation methods used. For performance confirmation of metrics related to probabilities of detection (Pd) and false alarm (Pfa), we used two types of validation information:

- For the small subset of data where there was overlapping MARS, vehicular, and HeliMag data, we used the vehicular data as ground truth and derived Pd and Pfa assuming the vehicular data to be perfect (Pd=1, Pfa = 0). Note: Since MARS is a WAA tool, we are not going to try to discriminate UXO from clutter, so false alarms are defined as picks where there are no metal targets detected by the ground vehicular data. We used a total-gradient detection algorithm on both the HeliMag and MARS data—the threshold was determined in the same manner as done earlier for HeliMag data at Pueblo. In this procedure we plotted the number of targets versus threshold—this plot has an inflection point where we start to pick into the noise (i.e., at lower thresholds the number of targets selected increases radically).

- For regions with only MARS and HeliMag data, we conducted a similar analysis. Once the inflection point was determined for both systems, we compared the following:
  - Relative target density results (to determine usefulness of MARS relative to HeliMag)
  - The threshold of the actual inflection point (to compare system performance);

- For the ESTCP emplaced targets, we computed the Pd for a range of ordnance types based on the emplaced data.

Table 8 describes the performance metrics, confirmation criteria, and results.

Table 7. Performance Criteria.

Performance Criteria	Description	Type of Performance Objective
Technology usage	Ease of use and efficiency of operations. Relative ease of use relates to the ability to fly the aircraft at the prescribed altitude, ability to incorporate the sensors and DAS system on the aircraft platform. Relative efficiency relates to the ability to consistently meet performance objectives.	Primary/ Qualitative
Target feature definition	Dipole fit feature estimates (parameters) derived from data collected twice daily over calibration targets. Parameters are X,Y,Z, size, dipole orientation.	Primary/ Quantitative
Location accuracy	Predicted location of calibration items < 0.5 m from the calibration items (including daily and ESTCP calibration items)	Primary/ Quantitative
Navigational accuracy	Actual flight path < 2 m from planned flight path. If the pilot is unable to fly lines within specification, gaps in coverage will occur. With a 7-m swatch and a planned transect separation of 5 m, an appropriate specification is 2 m. At that tolerance, the left- and right-hand sensors on adjacent passes will overlap. If the adjacent pass is also 2 m in error, then a data gap will occur.	Secondary/ Quantitative
Anomaly detection/density distribution fidelity	Target detection probabilities/target density estimates relative to the HeliMag system	Primary/ Quantitative/ Qualitative
MARS survey area coverage	Actual number of acres surveyed as a percentage of planned number of survey acres: The percentage coverage will be determined by assuming that a gap in coverage is any area where the sensors are > 2 m apart or where the sensor height is > 4 m above ground level.	Secondary/ Quantitative
Operating parameters (altitude, speed ,daily production rates)	Statistical assessment of operating parameter. Expect mean values to be 2-3 m AGL; 68 knots (35 m/s); 400 acres/day.	Secondary/ Quantitative
System noise	Accumulation of basal noise levels from all contributing sources other than environmental sources. These sources include sensors and sensor platforms, mechanical motion noise, radio frequencies, etc. calculated by root mean square.	Secondary/ Quantitative
Data density/point spacing	(Number of sensor readings/sec)/ airspeed and cross-track data density; number of sensor survey lines/survey area width	Secondary/ Quantitative

Table 8. Expected Performance and the Confirmation Methods Employed.

Performance Metric	Confirmation Method	Expected Performance	Actual Performance
Technology usage	Field experience using technology during demonstration for ease of use; ability to meet performance objectives for relative efficiency.	Relative ease of use and efficiency	Due to weather conditions, this was not met.
Target feature definition	Statistical analysis of dipole fit parameters derived from data collected over the calibration line targets. These will be compared to HeliMag data collected over equivalent calibration items at the site during the WAA demonstration survey.	Bias and standard deviation of dipole fit parameters for each target are within 25% of HeliMag results.	Standard deviations (HeliMag in parentheses) Depth: 0.16 m (0.13 m) Size: 7 mm (7 mm) Angle: 3.9° (6.0°)
Location accuracy	Statistical analysis of calibration, seed, and ground-truth items	Better than 0.5 m (standard deviation)	0.23 m E, N on calibration 0.48 to 0.74 m on seed and ground truth
Probability of detection compared to HeliMag	Comparison with HeliMag data. Pd(MARS) will be compared to the Pd(HeliMag) and Pfa will be compared to vehicular data (see text).	Pd(MARS) > 0.90 Pd(HeliMag), Pfa < 0.5	Pd(MARS) ~0.7 to 0.8 Pd(HeliMag)
Probability of detection on emplaced items	(Number emplaced targets detected) / (total number emplaced targets)	Pd > 0.9 on 105-mm caliber and greater	Pd = 93% 155 mm Pd = 60% 105 mm Pd = 13% 105 HEAT
Navigational accuracy	By comparing actual GPS track of each line against planned flight-path	95% within 2 m	NA
MARS survey area coverage relative to HeliMag	The percentage of acreage surveyed relative to the planned coverage will be calculated in a GIS.	Coverage > 90% planned area	65% north area 83% south area
System noise	The system noise will be calculated using root mean square error and will be based on data collected at high altitude (>500 ft AGL).	<1 nT on all sensors	0.13 to 0.17 nT outer sensors; 0.45 to 0.67 nT inner sensors
Data density/point spacing	Calculated from statistical analysis of survey data. Will use mean values from areas without large gaps (> 5 m in width)	0.175 m along track 2 m cross track	0.261 m along track Could not calculate cross-track density
Operating parameters (altitude, speed, daily production rate)	Will use the GPS data to compute histograms and mean values of altitude and speed. Will use GIS to compute area covered each day (will exclude weather days and will pro-rate coverage if weather forces an early stop to surveying)	2-3 m AGL; 68 knots (35 m/s); 400 acres/day	2.27 m average AGL; 72.3 knots (37.2 m/s); 260 acres/day actual 450 acres/day prorated for weather

8.2 DETECTION PROBABILITY RELATIVE TO HELIMAG

Expected performance: Pd(MARS) > 0.90 Pd(HeliMag) at PFa = 0.5

Actual performance: Not met

For performance assessment, we compared the MARS (Figure 14) and HeliMag data (Figure 15) within the two subregions of the northern survey area (Areas 1 and 2 on the maps). Both these regions comprise part of a target area with high anomaly density and also contain subregions that had been previously surveyed with GEO-CENTERS (now SAIC) magnetometer towed-array system (Grids 1a, 1b, 1c, 2a, 2b and 3d).

Comparison of MARS and HeliMag density estimates

To compare the performance of the two airborne systems, we used an automatic peak detection routine applied to total-gradient images derived from each system. Figure 6 plots the number of MARS and HeliMag detections as a function of anomaly amplitude in the two areas used for performance comparison (Figures 7a and 8a show the corresponding MARS total-gradient images for areas 1 and 2 while Figures 7b and 8b show the corresponding HeliMag total-gradient images). Both systems show a steady increase in the number of detections as the amplitude is decreased to a certain point, after which there is a rapid rise in the number of detections. We aim to select a threshold just before this inflection point in number of detections. It is evident that the inflection point needs to be selected using subjective criteria. However, two things are clear: (1) the HeliMag has a larger number of high amplitude targets (particularly for area 2), and (2) the inflection point for the HeliMag is lower than for the MARS. For both areas we decided to select a detection threshold of 3 nT/m for the HeliMag. For the MARS we selected a threshold that had the same slope as the HeliMag at 3 nT/m; these thresholds corresponded to 4.0 nT/m for Area 1 and 3.8 nT/m for Area 2.

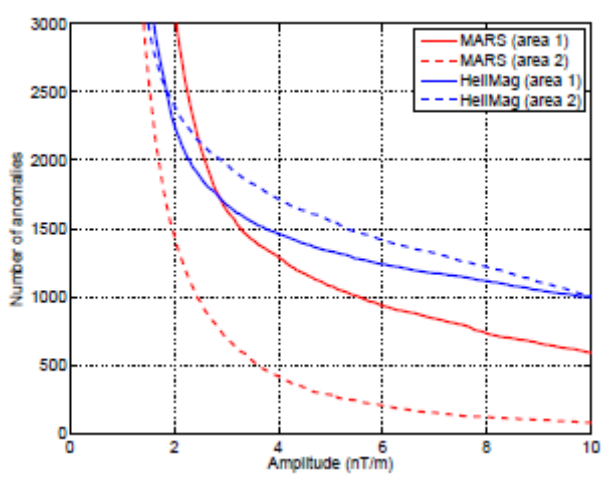

Figure 6. Number of MARS and Helimag Anomalies as a Function of Amplitude in Areas 1 and 2.

To estimate the distribution of metal objects across the study area, a density raster was computed using a 90-m radius neighborhood kernel that assigned anomaly densities in anomalies per hectare to each cell in the raster. The MARS and HeliMag density images in Area 1 are qualitatively similar (Figures 7c and d) in the southwesterly and southeasterly parts of the site. The MARS predicted densities are generally lower than the HeliMag, especially in the southwesterly corner. A point-by-point comparison of the anomaly densities (Figure 9a) reveals that the HeliMag predictions are on average 1.1 times the MARS predictions. After lowering the MARS target threshold to 3 nT/m (the same as the HeliMag), the predicted densities are in better agreement (Figures 7e and 9a), and the line of best fit has a slope of around 1. We conclude that in Area 1 the MARS and HeliMag technologies are comparable. A site manager would draw the same conclusions about the metal distribution across the survey area.

Turning now to Area 2, we see that the MARS and HeliMag density estimates are significantly different (Figures 8 and 9b). Figure 6 already revealed that there were many fewer detections in the MARS data compared to the HeliMag. Using a 3.8 nT/m threshold, the HeliMag densities are, on average, 3.75 times larger than those predicted by MARS. By reducing the MARS target threshold to 2 nT/m, the average discrepancy between predictions is reduced to 1.4 times the MARS density, but there is a large variation in the relative densities (presumably due to the significant number of false alarms at that threshold). Close inspection of the spatial distributions of the MARS and HeliMag densities reveals considerable discrepancies across the whole of Area 2. The differences are most pronounced in the target region to the far west of the area shown. From the HeliMag data the target area is predicted to be significantly larger and with a substantially higher concentration of metallic targets.

Systematic differences in the sensor elevation appear to be the main reason for the disparity in the predicted anomaly densities (Figure 10). On average, the MARS sensors were at about 2.42 m aboveground compared to 1.44 m for the HeliMag. The sensor ground clearance for both systems was significantly higher as the aircraft flew over a north-south oriented fence at about 150 m east. This presumably caused the depression in the HeliMag-derived density in the middle of the target area. The increase in sensor elevation lasted for about 50 m for the helicopter and closer to 100 m for the CT aircraft. In addition, the CT aircraft was flying higher as it approached the fence. Between about 130 and 180 m north, the MARS sensors were more than 4 m above the ground, and hence the data have been masked (too high for reliable detection). The higher elevations and longer recovery distance of the CT aircraft emphasizes a potential weakness of the MARS system when it encounters obstacles or sudden variations in terrain.

We conclude that in Area 2 the MARS-derived density estimates are inferior to the HeliMag-derived estimates, predominantly due to a higher survey altitude. The main target in the western part of the area is evident in the MARS data but has a smaller apparent footprint and metal concentration. In the lower density parts of the site, the HeliMag- and MARS-derived densities are poorly correlated. We suspect that areas of elevated concentration in the MARS data are due predominately to clusters of false alarms.

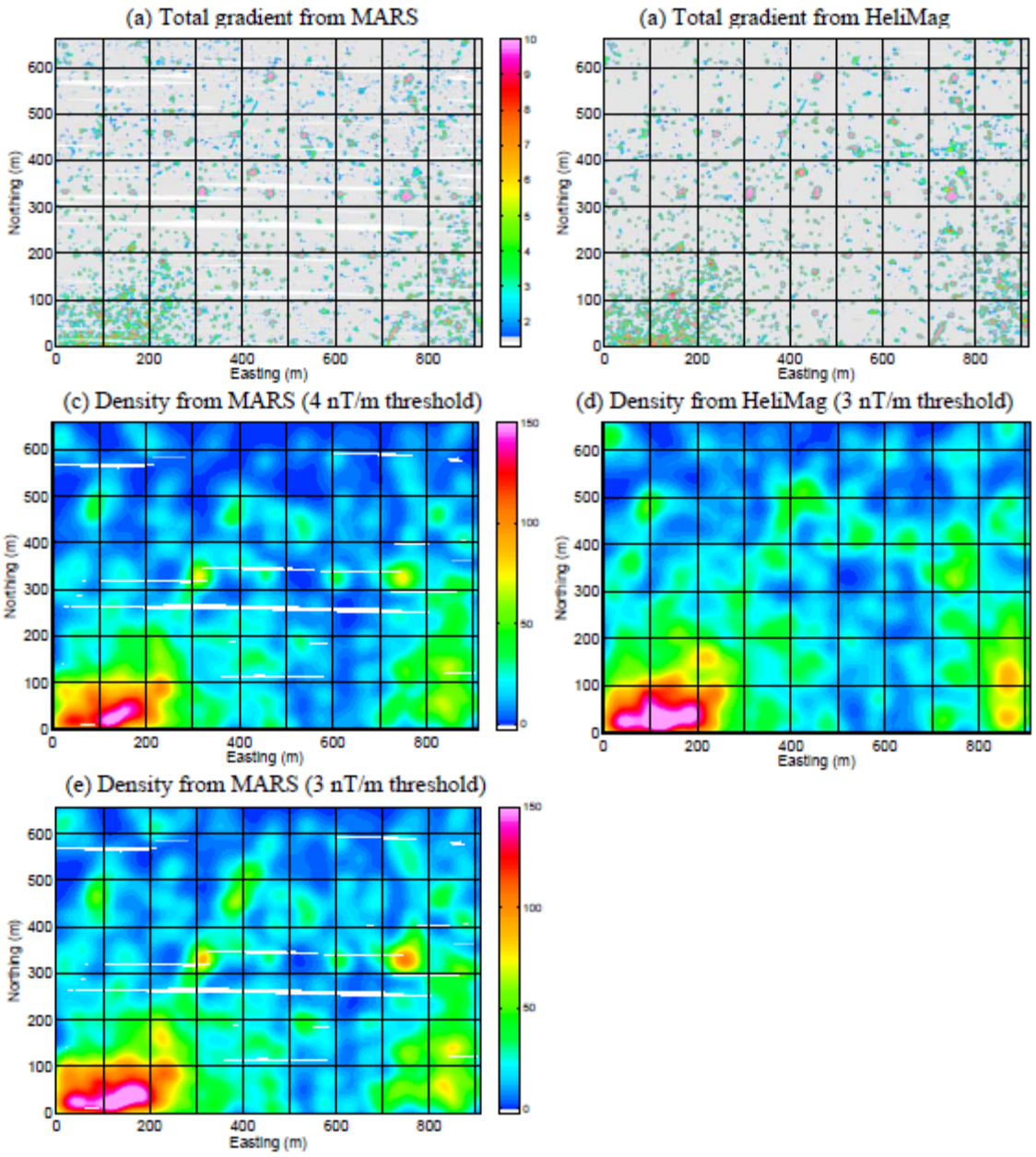

Figure 7. Comparison of MARS and HeliMag Densities in Area 1: (a) MARS Total Gradient Image, (b) HeliMag Total Gradient Image, (c) MARS Target Density with 4 nT/m Threshold, (d) HeliMag Target Density with 3 nT/m Threshold, and (e) MARS Target Density with 3 nT/m Threshold.

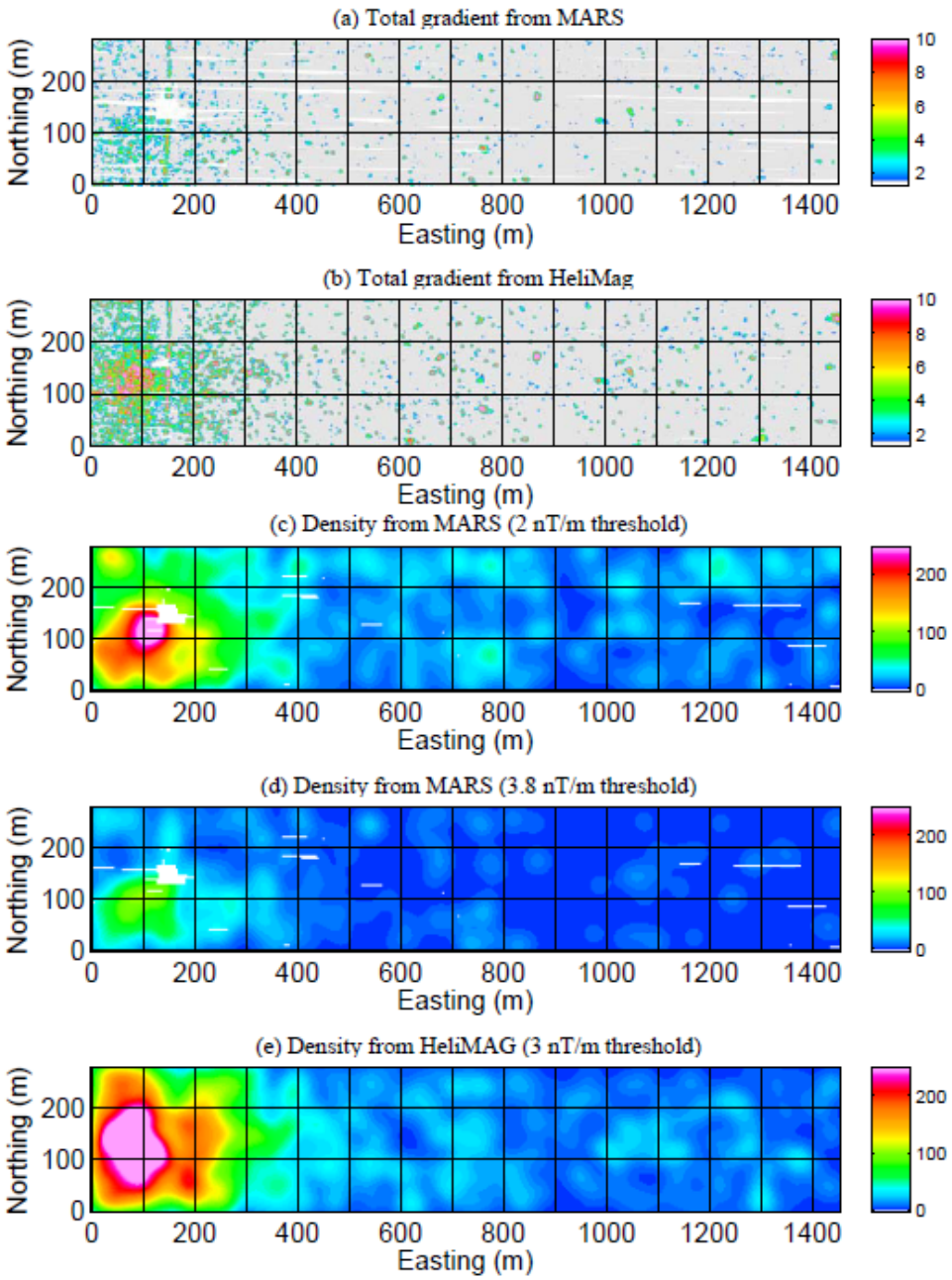

Figure 8. Comparison of MARS and HeliMag Densities in Area 2: (a) MARS Total Gradient Image, (b) HeliMag Total Gradient Image, (c) MARS Target Density with 2 nT/m Threshold, (d) MARS Target Density with 3.8 nT/m Threshold, and (e) HeliMag Target Density with 3 nT/m Threshold.

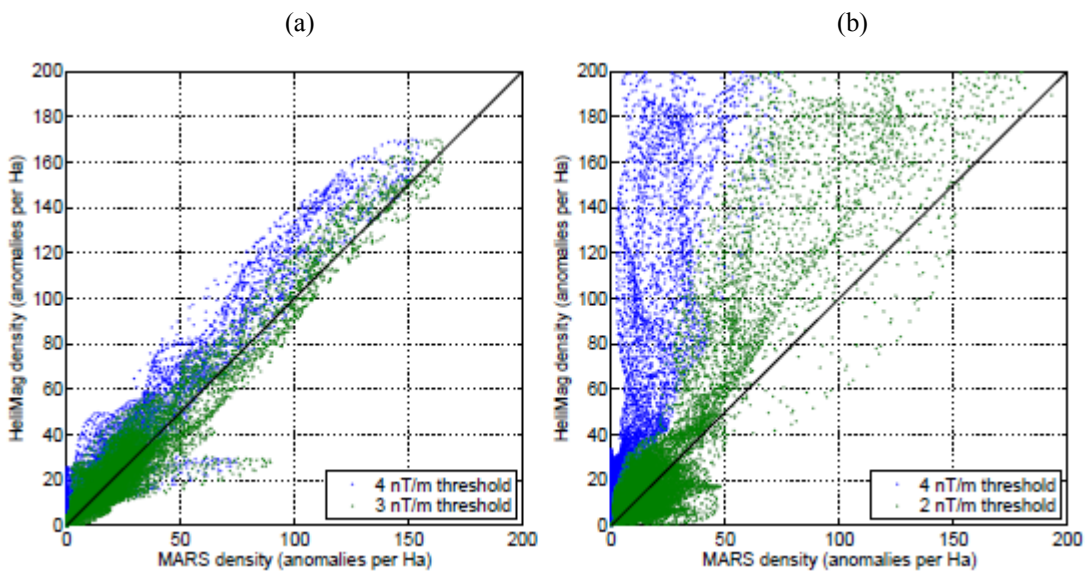

Figure 9. Point-By-Point Comparison of MARS and HeliMag Anomaly Densities in (a) Area 1 and (b) Area 2, Using Two Different Target Thresholds for the MARS Data.
(The solid black line represents a 1-1 relationship between densities.)

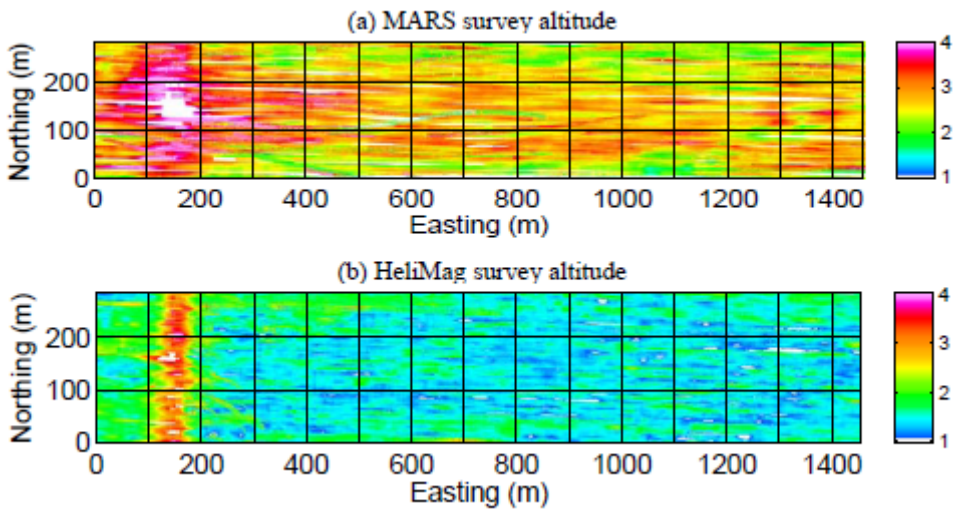

Figure 10. Comparison of MARS and HeliMag Sensor Elevations in Area 2.

Comparison of ground, MARS and HeliMag

We turn our attention now to the six subregions in Areas 1 and 2 that have coincident ground-based (GEO-CENTERS) magnetics, MARS, and HeliMag data. Figure 16 compares total-gradient images for each system over one of the subregions. Also included are total-gradient images for the ground-based system after upward continuation by 2.0 m. These upward continued images effectively represent the expected signal recorded by an airborne system flying at that elevation. Any item that causes a total-gradient signal above a certain threshold in the upward continued data should be detectable by an airborne system. We evaluate the performance of MARS and HeliMag using thresholds of 2 and 4 nT/m. These numbers bracket the inflection points evident in the plot of anomaly threshold versus number of anomalies (Figure 6).

Figure 11 shows receiver operating characteristic (ROC) curves for Areas 1 and 2 for the 2 nT/m and 4 nT/m threshold ground-truth data. The plots show the probability of detection against the number of false-alarms per acre. For the 2 nT/m ground-truth, the HeliMag target picks asymptote to Pd=0.9 at around five false alarms per acre, for both Area 1 and Area 2. For Area 1 the MARS Pd=0.7 at five alarms per acre and rises slowly to Pd=0.85 at 30 alarms per acre. MARS detection performance is significantly worse for Area 2, with Pd=0.6 at around five false alarms per acre, rising to Pd=0.8 at 20 false alarms per acre.

Considering only those ground-based anomalies with upward continued amplitudes greater than 4 nT/m, improves the HeliMag Pd to 0.95 and 0.93 in Areas 1 and 2 respectively. These detection probabilities are reached very quickly with false-alarm rates of 2.5 and 1 per acre, respectively. For Area 1, the MARS Pd=0.85 at five false-alarms per acre, rising to Pd=0.9 at 20 false alarms per acre. For Area 2, Pd=0.75 at five false alarms per acre, rising to Pd=0.83 at 18 false alarms per acre.

The MARS probabilities of detection are similar to those of the HeliMag data when upward continued by 1.0 m. The false alarm rates of these upward continued HeliMag are significantly smaller than those of MARS data. This is partly due to smoothing and elimination of noise by the upward continuation operation.

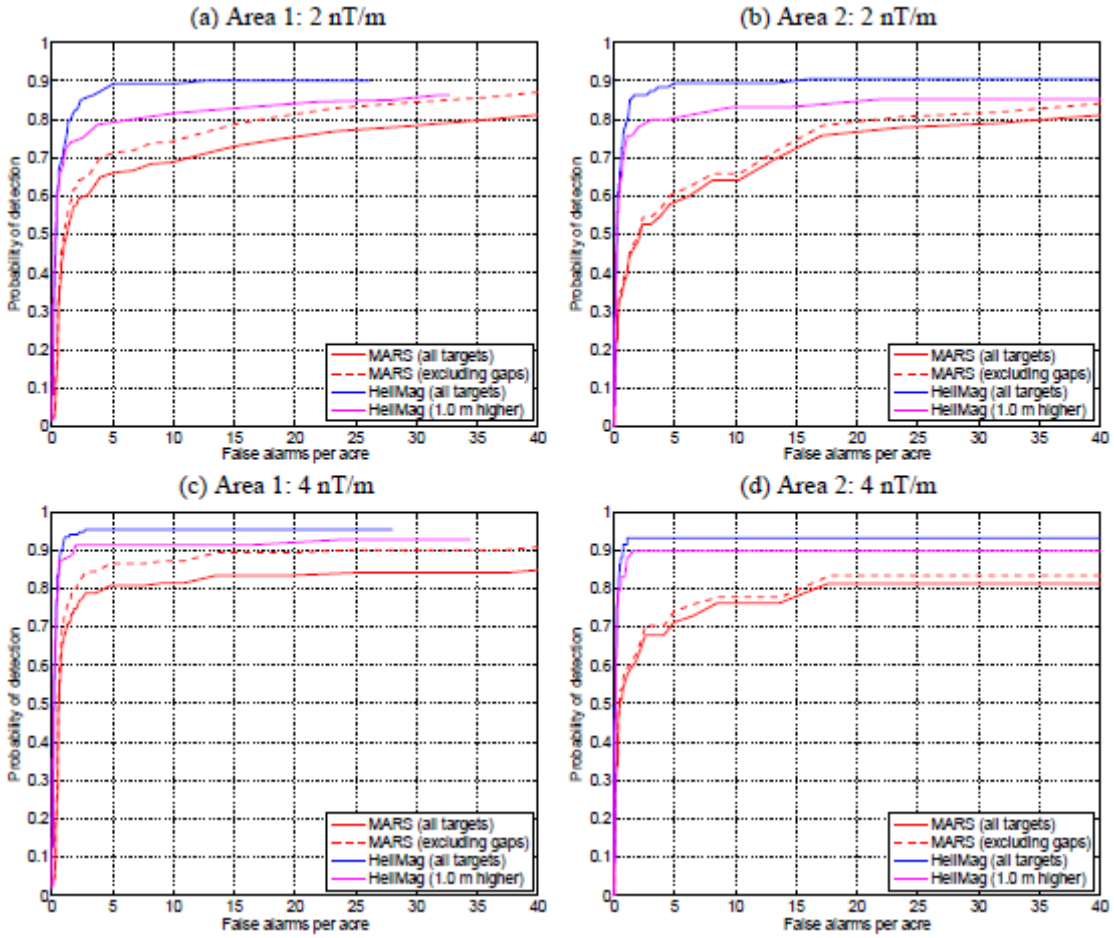

Figure 11. ROC Curves for the MARS and HeliMag Using the Ground-Based Data as Truth.

(Results are split between Area 1 [a and c] and Area 2 [b and d]. Targets were selected from the total-gradient of the ground-based data, upward continued by 2.0 m at thresholds of 2 nT/m [a and b] and 4 nT/m [c and d].)

9.0 COST ASSESSMENT

9.1 COST MODEL

Mobilization/demobilization, airborne surveys, processing, analysis, and reporting costs are summarized in Table 9. As noted, SeaTerra's data acquisition system and compensation system and SKY's magnetometers and GPS were deployed for this demonstration survey, and the daily rental costs for that equipment are reflected in the reported costs.

Table 9. Cost Tracking.

Cost Category	Sub Category	Details	Costs ($)
Start-up and coordination costs	Technology certification and installation	Includes project start-up, sensor boom engineering and fabrication, coordination with FAA and aircraft manufacturer for approval of aircraft modifications, installation	81,218(certification, installation) 9,467(planning documents)
	Premobilization testing	Tests conducted December 2006 and April 2007	54,589
	Site visit and coordination	Coordination, travel for site visit to KPBR and Pueblo of Isleta	6,380
	Mobilization	Personnel, equipment, and aircraft mobilization costs—Ashland, OR, to Albuquerque, NM	28,897
Operating costs	Demonstration survey	Data acquisition and associated tasks, including CT operation time, project team per diem, equipment and subcontract costs, 18 days on site	132,769
	Data processing	Initial and secondary processing of data (including on-site processing)	63,733
	Data analysis	Analysis of MARS data	16,018
Demobilization		Personnel, equipment, and aircraft mobilization costs—Albuquerque, NM, to Ashland, OR	11,219
Other costs	Demonstration report preparation		21,106(est)
	Management and reporting	Project related management, reporting, and contracting. Costs include In-Progress Reviews (IPR), symposium attendance	62,500
		Total Demonstration Cost	487,896
		Acres Characterized	2795
		Demonstration cost per acre	174.56/acre

Estimated costs for a production survey

9.2 COST DRIVERS

The cost of an airborne survey depends on many factors, including:

- Aircraft costs, which can vary, depending on the provider of the aircraft
- Length and number of flight lines required to survey the area

- Climate and weather conditions, which can affect productivity
- Location of the site, which can influence the cost of logistics
- Amount of analysis required to sufficiently review the data.

Aircraft costs are a major cost factor for any airborne survey. Significant variables and factors associated with the mobilization, data acquisition, and demobilization costs include the cost of aircraft time and standby time. The cost of aircraft can vary depending upon the type of aircraft and operating costs. Standby time can also influence the cost of a survey and is typically assessed at the cost of one day of data collection (minimum of 4 hours were used for these demonstrations), including aircraft costs, labor, and travel. For multiday surveys, weather can be more of a variable, and standby time can increase costs.

Mobilization and demobilization costs are most significantly a function of the distance from the home base for the aircraft. In addition to the cost of mobilizing and demobilizing the aircraft, the cost of mobilizing equipment (sensors and GPS equipment) can add significantly to costs. For longer mobilization distances, the costs of equipment rental for mobilization and demobilization can be substantial. Therefore, for a site requiring a longer mobilization distance, the mobilization and demobilization can take up a correspondingly larger amount of the budget, especially for a relatively small site.

Data processing and analysis costs are generally linear with project size and site complexity; other influential factors include the objectives of the program and associated data requirements. Processing costs and data deliverable times have been decreasing with experience at multiple sites, automation of processing and analysis routines, and increased computing power resulting in faster processing.

The costs reported in Table 9 are for the demonstration and would be significantly higher than a production survey with the MARS system. Table 10 presents a comparison of MARS and HeliMag costs for a range of survey sizes and mobilization distances; all scenarios assume data collection rates of 250 acres/day. The costs for planning, document preparation, management, and data processing were assumed to be equivalent for the two technologies. As would be expected, the cost differences occur in the survey and mobilization costs, mostly caused by the difference in aircraft operations costs, and to a lesser extent, equipment costs. Table 11 is a summary of the comparison and shows that the MARS costs would range from 51% to 66% of the HeliMag costs for the various survey sizes and mobilization distances.

Assumptions for the MARS production survey costs include:

- Four-person site team, including CT pilot, geophysicist, geophysical technician/ground control support, and aircraft mechanic. Costs include labor and per diem.

- Mobilization and demobilization travel days, 1 day each for installation and testing and deinstallation for the site team.

- Aircraft operations assume a rate of $160/hour with a minimum 4 hours/day. Based on the KPBR demonstration, a data collection rate of 90 acres/hour is a

reasonable average for days without significant weather issues. Therefore, for the cost comparison, the $640/day minimum was assumed.

The volume of data collected and processing were assumed to be equivalent to that for HeliMag considering the standardized data collection rate and number of days onsite.

9.3 COST BENEFIT

The benefits of low-level magnetometer surveys for wide area assessment purposes have been established and discussed thoroughly elsewhere (e.g., "Demonstration of Helicopter Multi-Towed Array Detection System (MTADS) Magnetometry Technology for the ESTCP Wide Area Assessment Pilot Program" Cost and Performance Report, Sky Research, 2008). This demonstration project has shown that MARS performance is generally inferior to HeliMag but that the costs are between 51 to 66% of a HeliMag survey. In the flat, open areas of Kirtland, MARS survey altitudes and detection performance were comparable to that of HeliMag. Therefore, in those types of areas, MARS could substitute for HeliMag and potentially reduce survey costs. In areas with more topographic complexity, MARS survey altitudes and performance were significantly worse than that of HeliMag, and MARS was not an adequate substitute.

The niche for MARS appears to be in flat, open sites with larger (105 mm or greater) caliber munitions, particularly when those sites are relatively small because then a MARS survey is a much cheaper alternative than HeliMag.

Table 10. MARS-HeliMag Cost Comparison.

Survey Size: 1,000 Acres								
4 hr each way to mob/demob			**8 hr each way to mob/demob**			**16 hr each way to mob/demob**		
	HeliMag	**MARS**		**HeliMag**	**MARS**		**HeliMag**	**MARS**
Planning, prep, & project mgt (including work plans)	$32,000	$32,000	Planning, prep, & project mgt (including work plans)	$32,000	$32,000	Planning, prep, & project mgt (including work plans)	$32,000	$32,000
Mob/demob/install boom	$40,000	$27,128	Mob/demob/install boom	$72,000	$31,351	Mob/demob/install boom	$110,000	$42,133
Survey	$82,000	$35,904	Survey	$82,000	$35,904	Survey	$82,000	$35,904
Data processing & analysis	$12,000	$12,000	Data processing & analysis	$12,000	$12,000	Data processing & analysis	$12,000	$12,000
Final report	$12,000	$12,000	Final report	$12,000	$12,000	Final report	$12,000	$12,000
Total	**$178,000**	**$119,032**	**Total**	**$ 210,000**	**$123,255**	**Total**	**$248,000**	**$134,037**
Cost Per Acre	**$178**	**$119**	**Cost Per Acre**	**$ 210**	**$123**	**Cost Per Acre**	**$248**	**$134**
Survey Size: 5,000 Acres								
4 hr each way to mob/demob			**8 hr each way to mob/demob**			**16 hr each way to mob/demob**		
	HeliMag	**MARS**		**HeliMag**	**MARS**		**HeliMag**	**MARS**
Planning, prep, & project mgt (including work plans)	$47,000	$47,000	Planning, prep, & project mgt (including work plans)	$47,000	$47,000	Planning, prep, & project mgt (including work plans)	$47,000	$47,000
Mob/demob/install boom	$40,000	$27,128	Mob/demob/install boom	$72,000	$31,351	Mob/demob/install boom	$110,000	$42,133
Survey	$410,000	$179,520	Survey	$410,000	$179,520	Survey	$410,000	$179,520
Data processing & analysis	$40,000	$40,000	Data processing & analysis	$40,000	$40,000	Data processing & analysis	$40,000	$40,000
Final report	$15,000	$15,000	Final report	$15,000	$15,000	Final report	$15,000	$15,000
Total	**$552,000**	**$308,648**	**Total**	**$584,000**	**$312,871**	**Total**	**$622,000**	**$323,653**
Cost Per Acre	**$110**	**$62**	**Cost Per Acre**	**$117**	**$63**	**Cost Per Acre**	**$124**	**$65**
Survey Size: 7,500 Acres								
4 hr each way to mob/demob			**8 hr each way to mob/demob**			**16 hr each way to mob/demob**		
	HeliMag	**MARS**		**HeliMag**	**MARS**		**HeliMag**	**MARS**
Planning, prep, & project mgt (including work plans)	$55,000	$55,000	Planning, prep, & project mgt (including work plans)	$55,000	$55,000	Planning, prep, & project mgt (including work plans)	$55,000	$55,000
Mob/demob/install boom	$40,000	$27,128	Mob/demob/install boom	$72,000	$31,351	Mob/demob/install boom	$110,000	$42,133
Survey	$612,000	$269,280	Survey	$612,000	$269,280	Survey	$612,000	$269,280
Data processing & analysis	$54,000	$54,000	Data processing & analysis	$54,000	$54,000	Data processing & analysis	$54,000	$54,000
Final report	$20,000	$20,000	Final report	$20,000	$20,000	Final report	$20,000	$20,000
Total	**$781,000**	**$425,408**	**Total**	**$813,000**	**$429,631**	**Total**	**$851,000**	**$440,413**
Cost Per Acre	**$104**	**$57**	**Cost Per Acre**	**$108**	**$57**	**Cost Per Acre**	**$113**	**$59**

Table 10. MARS-HeliMag Cost Comparison (continued).

Survey Size: 10,000 Acres								
4 hr each way to mob/demob			**8 hr each way to mob/demob**			**16 hr each way to mob/demob**		
	HeliMag	**MARS**		**HeliMag**	**MARS**		**HeliMag**	**MARS**
Planning, prep, & project mgt (including work plans)	$62,000	$62,000	Planning, prep, & project mgt (including work plans)	$62,000	$62,000	Planning, prep, & project mgt (including work plans)	$62,000	$62,000
Mob/demob/install boom	$40,000	$27,128	Mob/demob/install boom	$72,000	$31,351	Mob/demob/install boom	$110,000	$42,133
Survey	$816,400	$359,040	Survey	$816,400	$359,040	Survey	$816,400	$359,040
Data processing & analysis	$67,000	$67,000	Data processing & analysis	$67,000	$67,000	Data processing & analysis	$67,000	$67,000
Final report	$30,000	$30,000	Final report	$30,000	$30,000	Final report	$30,000	$30,000
Total	**$1,015,400**	**$545,168**	**Total**	**$1,047,400**	**$549,391**	**Total**	**$1,085,400**	**$560,173**
Cost Per Acre	**$102**	**$55**	**Cost Per Acre**	**$105**	**$55**	**Cost Per Acre**	**$109**	**$56**

Table 11. MARS-HeliMag Cost Comparison Summary.

Survey Area (Acres)	4 Hr Mob/Demob			8 Hr Mob/Demob			16 Hr Mob/Demob		
	HeliMag ($/Acre)	MARS ($/Acre)	Mars/HeliMag Cost (%)	HeliMag ($/Acre)	MARS ($/Acre)	Mars/HeliMag Cost (%)	HeliMag ($/Acre)	MARS ($/Acre)	Mars/HeliMag Cost (%)
1,000	178	119	**66.9**	210	123	**58.6**	248	134	**54.0**
5,000	110	62	**56.4**	117	63	**53.8**	124	65	**52.4**
7,500	104	57	**54.8**	108	57	**52.8**	113	59	**52.2**
10,000	102	55	**53.9**	105	55	**52.4**	109	56	**51.3**

This page left blank intentionally.

10.0 REFERENCES

Billings, S. D., C. Pasion, S. Walker, and L. Beran. 2006. Magnetic models of unexploded ordnance: IEEE Transactions of Geoscience and Remote Sensing, 44, 2115- 2124.

Blakely, R. J. 1996. Potential Theory in Gravity and Magnetic Applications. Cambridge University Press.

Blakely, R.J., and R. W. Simpson. 1986. Approximating edges of source bodies from magnetic or gravity anomalies. Geophysics, v.51, p.1494-1498.

Sky Research, Inc. 2008. Demonstration of Helicopter Multi-Towed Array Detection System (MTADS) Magnetometry Technology for the ESTCP Wide Area Assessment Pilot Program Cost and Performance Report. Final. June.

Versar. 2005. Former Kirtland Precision Bombing Range, Conceptual Site Model, V0.

This page left blank intentionally.

APPENDIX A

POINTS OF CONTACT

Point of Contact	Organization	Phone Fax E-Mail	Role
Dr. Stephen Billings	Sky Research, Inc. 112A/ 2386 East Mall Vancouver, BC, V6T 1Z3 Canada	Phone: 541-552-5185 Cell: 604-506-9206	Co-Principal Investigator
David Wright	Sky Research, Inc. 9500 Kingsford Drive Cary, NC 27511	Phone: 541-633-5255	Co-Principal Investigator
Edgar Schwab	SeaTerra GMBH	Phone: 49-160-471-5580	Research Partner
Ms. Joy Rogalla	Sky Research, Inc. 445 Dead Indian Road Ashland, OR 97520	Phone: 541-552-5104	Project Manager
Mr. Scott Millhouse	USACE Engineering and Support Center Huntsville Box 1600 Huntsville, AL 35807-4301	Phone: 256-895-1607	Contracting Officer Technical Representative

This page left blank intentionally.

APPENDIX B

SELECTED IMAGES OF GROUND, MARS, AND HELIMAG DATA

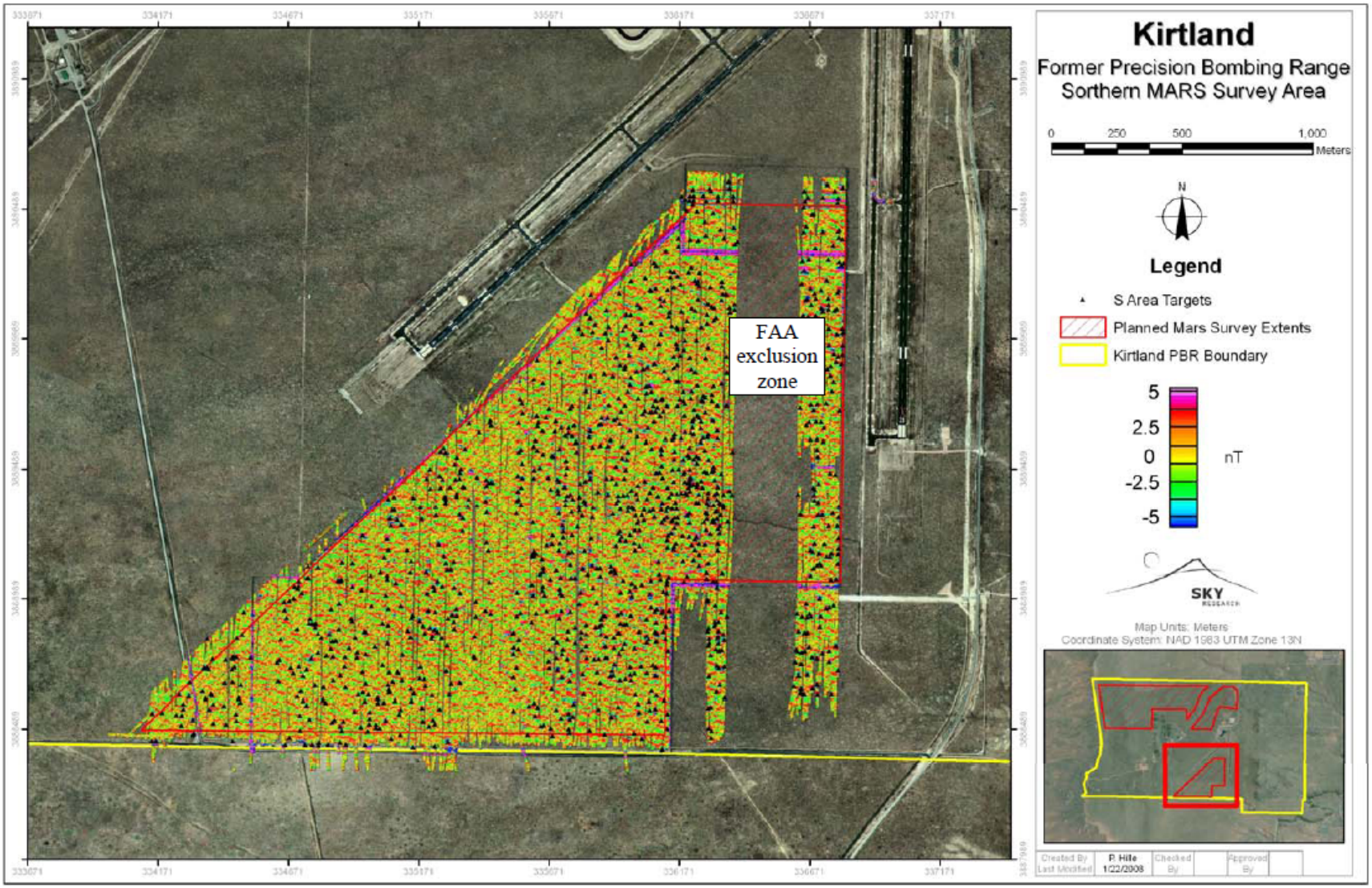

Figure 12. KPBR MARS Survey Southern Area Total-Field Anomaly Map with Manually Selected Targets Overlain.

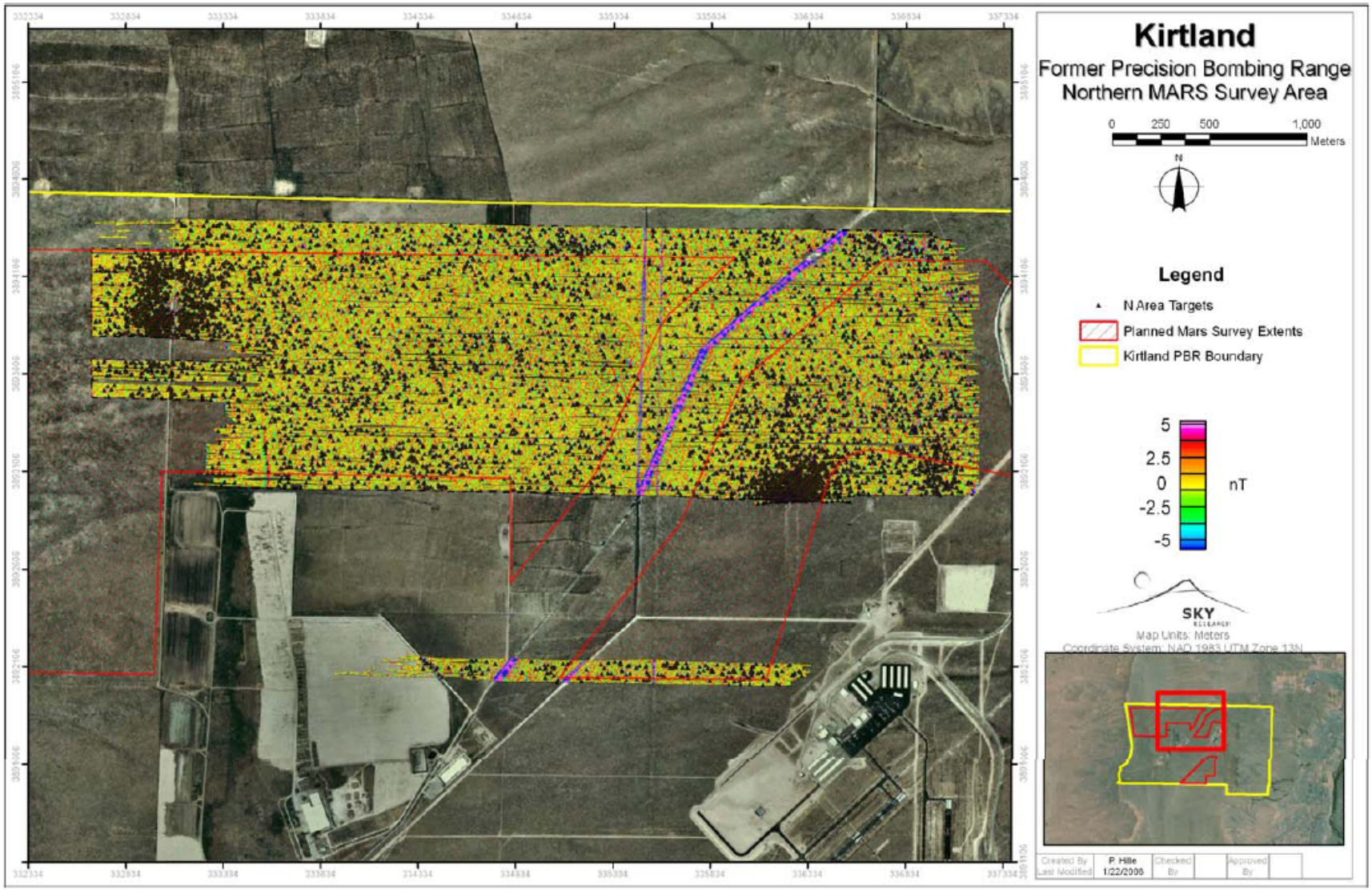

Figure 13. KPBR MARS Survey Northern Area Total-Field Anomaly Map with Manually Selected Targets Overlain.

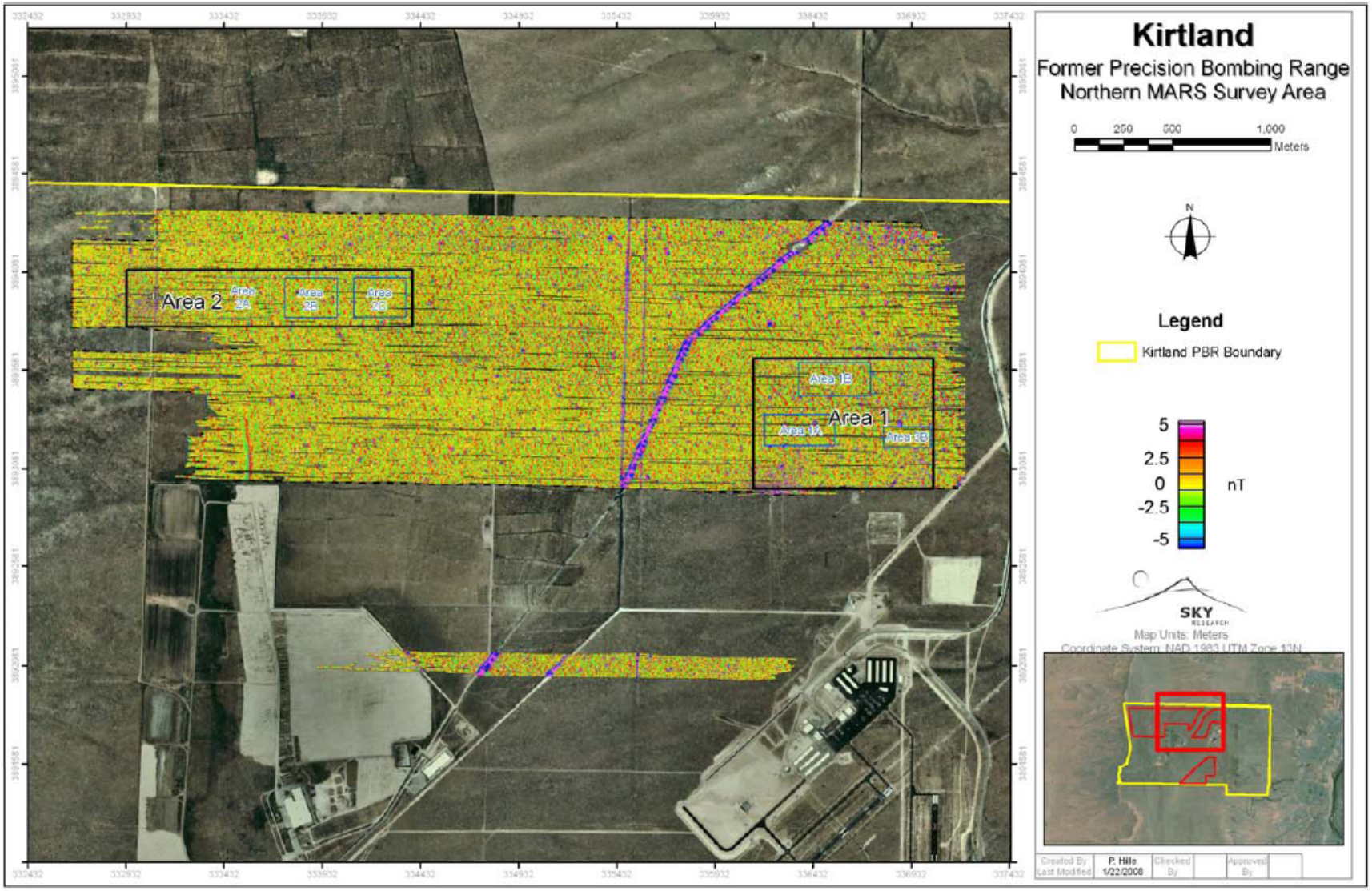

Figure 14. Map Showing the Location of the Two Areas Selected for Comparison of the MARS, HeliMag, and Ground-Based Datasets.

(There were six different areas covered with the ground-based system [shown as green rectangles].)

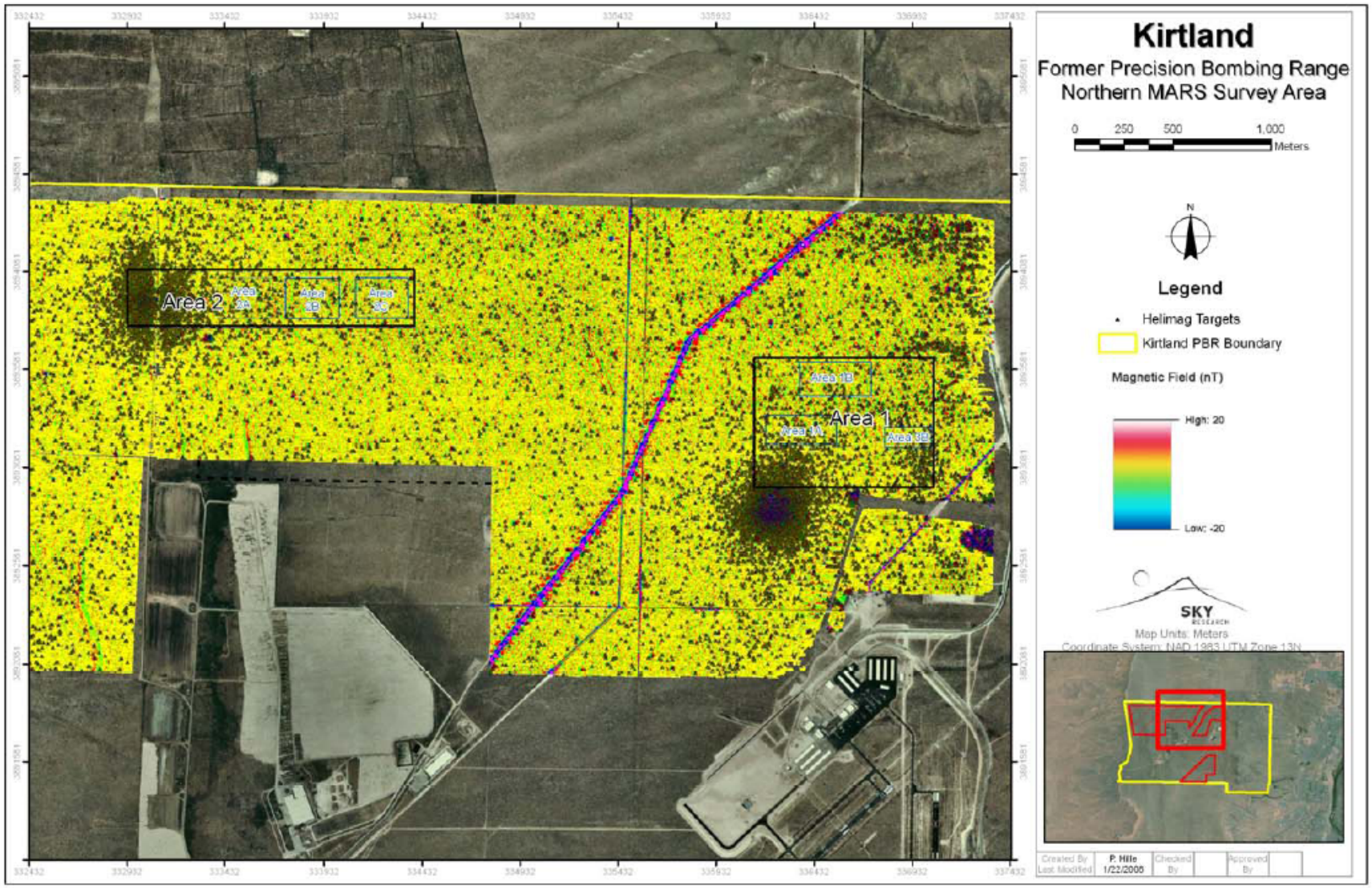

Figure 15. Total-Field Data from a Previous HeliMag Survey of the Northern Part of the KPBR Site with Manually Selected HeliMag Anomalies Overlain.

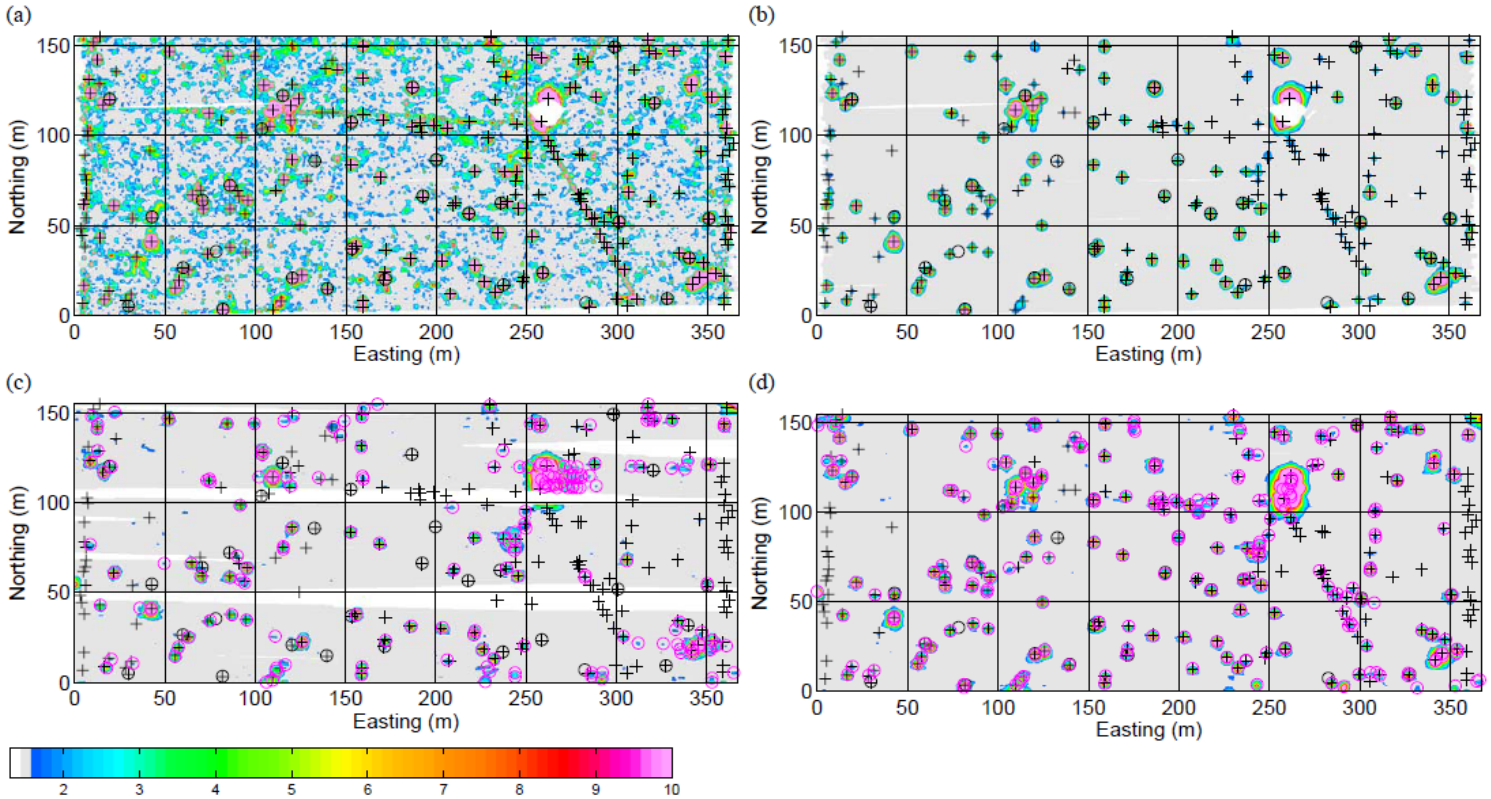

Figure 16. Comparison of (a) Ground-Based, (b) Upward Continued Ground-Based (2 m), (c) MARS, and (d) HeliMag Data on Grid 1a.

(All images are total-gradient with the same color-stretch. Ground-based targets are plotted as black-crosses; excavation locations are plotted as black circles, and MARS and HeliMag target picks are plotted as magenta circles; the targets along the linear magnetic feature and the western edge were excluded from the performance analysis.)

ESTCP Program Office

901 North Stuart Street
Suite 303
Arlington, Virginia 22203

(703) 696-2117 (Phone)
(703) 696-2114 (Fax)

E-mail: estcp@estcp.org
www.estcp.org